



*Division head Marcel Verheij*

**Marcel Verheij MD PhD** Head

**Berthe Aleman MD PhD** Academic staff

**Harry Bartelink MD PhD** Academic staff

**José Belderbos MD PhD** Academic staff

**Monique Bloemers MD** Academic staff

**Eugène Damen PhD** Academic staff

**Roel de Boer PhD** Academic staff

**Luc Dewit MD PhD** Academic staff

**Paula Elkhuizen MD PhD** Academic staff

**Rick Haas MD PhD** Academic staff

**Olga Hamming-Vrieze MD** Academic staff

**Wilma Heemsbergen PhD** Academic staff

**Frank Hoebbers MD PhD** Academic staff

**Edwin Jansen MD PhD** Academic staff

**Joost Kneijens MD** Academic staff

**Han Krewinkel MSc** Academic staff

**Joos Lebesque MD PhD** Academic staff

**Ben Mijnheer PhD** Academic staff

**Luc Moonen MD PhD** Academic staff

**Arash Navran MD** Academic staff

**Heike Peulen MD** Academic staff

**Floris Pos MD PhD** Academic staff

**Coen Rasch MD PhD** Academic staff

**Babs Reichgelt MD** Academic staff

**Peter Remeijer PhD** Academic staff

**Nicola Russell MD PhD** Academic staff

**Govert Salverda MD** Academic staff

**Christoph Schneider PhD** Academic staff

**Jan-Jakob Sonke PhD** Academic staff

**Joep Stroom PhD** Academic staff

**Marcel van Herk PhD** Academic staff

**Baukelien van Triest MD PhD** Academic staff

**Karijn Verschuere MD** Academic staff

**Corine van Vliet-Vroegindeweyj PhD** Academic staff

**Thelma Witteveen MD PhD** Academic staff

**Frits Wittkämper PhD** Academic staff

**Gerben Borst MD PhD** Temporary staff

**Mieke Harrick MD** Temporary staff

**Birgit Hollmann MD** Temporary staff

**Monique de Jong MD** Temporary staff

**Philip Meijnen MD PhD** Temporary staff

**Stella Mook MD** Temporary staff

**Marlies Nowee MD PhD** Temporary staff

**Brenda Tomaso MD** Temporary staff

**Femke van der Leij MD** Temporary staff

**Wouter Vogel MD PhD** Temporary staff

**Ben Vanneste MD** Temporary staff

**Brian Vendel MD** Temporary staff

**Francine Voncken MD** Temporary staff

**Tanja Alderliesten PhD** Post-doc

**Chun Chen PhD** Post-doc

**Alessia Gasparini PhD** Post-doc

## DIVISION OF RADIOTHERAPY

In 2010, our research activities continued to focus on: (1) improving treatment accuracy by optimal dose distribution, geometrical precision and dosimetric treatment verification, (2) enhancing radiation response by altered fractionation schedules, chemoradiation and biological response modifiers, and (3) predicting treatment response and prognosis by genetic profiling, functional imaging and biomarkers.

Adaptive strategies (ART) and volumetric rotational radiation delivery (VMAT) have become standard of care in an increasing number of indications. The in-house developed 3-dimensional EPID dosimetry is now available for all curatively and radically treated patients and ensures the safe delivery of the radiation dose. This innovation ranked third in the National Patient Safety Contest. As a direct result of these technological advances, extremely hypofractionated regimens such as stereotactic body radiotherapy (SBRT) have become a valuable alternative to surgery for early stage disease and oligometastases. To increase patient comfort during irradiation, one of our treatment suites was equipped with a technology that provides a personalized visual and acoustic ambience, which is expected to have a positive impact on patient convenience and stability. An increasing number of targeted agents find their way to the clinic as potential radiosensitizers. Recently established collaborations with pharmaceutical companies have resulted in new combined modality initiatives. To aid the preclinical identification of promising agents and their optimal scheduling, we have acquired an image-guided microbeam irradiator for small animals, integrated in the mouse cancer clinic facility. Functional imaging like FDG-PET and fMRI is increasingly used in our treatment planning protocols and allows a better prediction of response. New prognostic/predictive genetic profiles are being explored in early stage laryngeal and breast cancer, contributing to a more customized therapeutic approach.

In 2010 the division had its quinquennial scientific site visit. An international panel of experts qualified the division as an international leader in the field of radiotherapy with a very impressive scientific program. Useful recommendations will be worked out in the coming years.

In September 2010, the third scientific meeting of the Descartes Cancer Consortium was organized by the Karolinska Institutet, Sweden. This collaboration of three European cancer centers (Institut Gustave Roussy, Karolinska Institutet and NKI-AVL) was founded in 2008 to provide a platform of complementary expertise for conducting early clinical trials with an emphasis on novel targeted agents. Three trials are now running simultaneously at the three institutes.

The Radiotherapy department remains an active proponent of introducing proton therapy in The Netherlands and collaborates with Erasmus MC, Leiden University MC and TU Delft within the Holland Therapy Center (HollandPTC) consortium. Four co-workers of the division successfully defended their theses: Edwin Jansen (chemoradiotherapy in gastric cancer), Dimitry Nuyten (gene expression profiling in breast cancer), Monique Smitsmans (IGRT of prostate cancer) and Marcel Steggerda (prostate brachytherapy).

## IMAGE ACQUISITION AND PROCESSING

Tanja Alderliesten Suzanne van Beek, Anja Betgen, Johan de Boer, Roman Bohoslavsky, Kristy Brock, Niel Burnett, Richard Clarkson<sup>1</sup>, Hermine Dees-Ribbers, Andre Dekker, Joop Duppen, Alessia Gasparini, Rick Haas, Rutger Heddes, Maarten Hulshof, Rianne de Jong, Vincent Khoo<sup>1</sup>, Simon van Kranen, Philippe Lambin<sup>2</sup>, Joos Lebesque, Patricia Lindsay<sup>1</sup>, Corrie Marijnen, Angelo Mencarelli, Cathryn Nagel, Thao-Nguyen Nguyen, Jasper Nijkamp, Steven Petit, Lennert Ploeger, Floris Pos, Coen Rasch, Theo de Reijke<sup>3</sup>, Peter Remeijer, Simon Rit, Peter de Ruiter, Sarah Swift, Rajko Topolnjak, Corine van Vliet-Vroegindeweij, Marnix Witte, Lambert Zijp, Jan-Jakob Sonke, Marcel van Herk

<sup>1</sup> The Royal Marsden NHS, London, UK

<sup>2</sup> MAASTRO clinic, Maastricht, The Netherlands

<sup>3</sup> Free University of Amsterdam, The Netherlands

### TARGET VOLUME DEFINITION

#### Microscopic disease extension in 3D for Non Small Cell Lung Cancer: development of a prediction model using pathology validated PET/CT features

In radiotherapy planning of non-small cell lung cancer (NSCLC), uncertainties exist concerning the clinical target volume (CTV), meant to cover potential microscopic disease extension (MDE) around the visible tumor. The aim of the current study was to establish pre-treatment risk factors for the presence of MDE. The total tumor-bearing region at pathology is called CTVpath. 34 NSCLC patients, who underwent CT and PET prior to lobectomy, were included. The specimen was examined microscopically for MDE and image based prediction model was developed for the presence of MDE. MDE was found in 17 of the 34 patients (50%). After deformation correction, MDE was less than 26 mm in 90% of patients. A two-parameter model (mean tumor density and tumor volume on CT) predicted the presence of MDE (AUC: 0.86). 13 patients (38%, 95% CI: 24-55%) were identified as low risk for MDE, being potential candidates for reduced intensity therapy around the GTV. In the low risk group, the effective diameter of the GTVCT/PET accurately represented the diameter of the CTVpath. In the high-risk group, CT and PET underestimated the CTVpath by 2-3 cm. In conclusion, CT and PET accurately visualize the CTVpath in low risk patients, but underestimate the CTVpath in high-risk patients.

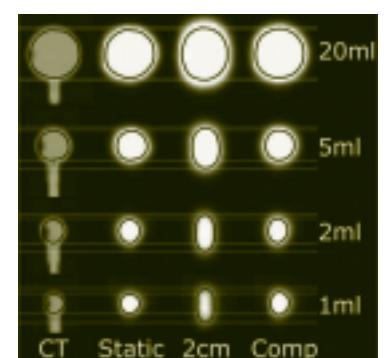
#### Validation of a mid-position PET scan for treatment planning in radiotherapy

Recently, respiratory correlated PET/CT (4D-PET) became commercially available. While 4D-PET reduces respiratory induced blurring, noise is increased since each phase uses fewer counts. We previously developed mid-position (MidP) CT reconstruction technique (motion compensated CT) for 3D radiotherapy planning using deformable image registration. To improve the quality of our PET data we developed a similar technique for 4D PET. 4D PET/CT scans of a dynamic respiration phantom were taken on a Philips Gemini 16. The phantom contained four spheres of different sizes (20 ml, 5 ml, 2 ml and 1 ml). The phantom moved with amplitudes ranging from 0 to 2 cm. To compensate for motion in the PET, we determined the motion from the 4D CT. Subsequently all voxels in the PET scan are relocated to the local mean position of the CT motion trajectory. After this, the 4D PET dataset is averaged, resulting in a 3D MidP PET dataset. To validate this method, we compared the uncompensated and the motion compensated PET data for maximum and mean intensity in the spheres ( $I_{max}$  and  $I_{mean}$ ) and the apparent sphere size. Compared to a static situation, a motion amplitude of 2 cm reduced  $I_{max}$  largely (ranging 6% for the 20 ml to 56% for the 1 ml sphere). Motion compensation reduced the loss of intensity by about 50%. Motion also increased the apparent size of the spheres. For instance, an amplitude of 2 cm increased the estimated size of the 5 ml sphere by 37%. After motion compensation, the size restored to within 2%. The MidP PET is expected to improve PET based radiotherapy planning (figure 1).

## Publications (continued)

Marnix Maas PhD Post-doc  
 Anton Mans PhD Post-doc  
 Vanessa Mexner PhD Post-doc  
 Anke van Mourik PhD Post-doc  
 Raul Pecharrroman Gallego PhD Post-doc  
 Simon Rit PhD Post-doc  
 Roel Rozendaal PhD Post-doc  
 Alize Scheenstra PhD Post-doc  
 Hanno Spreeuw PhD Post-doc  
 Rajko Topolnjak PhD Post-doc  
 Markus Wendling PhD Post-doc  
 Marnix Witte PhD Post-doc  
 Barry Doodeman Physician assistant  
 Marcel Jonker Physician assistant  
 Robin Kalisvaart Physician assistant  
 Margriet Kwint Physician assistant  
 Sandra Vreeswijk Physician assistant  
 Anja Betgen MSc Technical staff  
 Josien de Bois Technical staff  
 Joop Duppen Technical staff  
 Joeri Honnef Technical staff  
 Rianne de Jong Technical staff  
 Angelo Mencarelli Technical staff  
 Tom Minderhoud Technical staff  
 Danny Minkema Technical staff  
 Agnieszka Olszewska MSc Technical staff  
 Carmen Panneman MSc Technical staff  
 Carolien Peters Technical staff  
 Kenneth Pengel MSc Technical staff  
 Lennert Ploeger Technical staff  
 Maddalena Rossi MSc Technical staff  
 René Tielenburg Technical staff  
 Lambert Zijp MSc Technical staff

Figure 1: Depictions of the sphere with PET-based delineations (based on 40% of  $I_{max}$ ). The spheres were moving vertically. It can be seen that the shape of the object in the PET image is improved after motion compensation. (CT = CT-data, Static = PET with no amplitude, 2 cm = PET with 2 cm amplitude. Comp = Motion compensated PET)



## Publications

Alderliesten T, Loo C, Paape A, Muller S, Rutgers E, Peeters MJ, Gilhuijs K. *On the feasibility of MRI-guided navigation to demarcate breast cancer for breast-conserving surgery. Med Phys* 2010;37:2617-26

Aleman BM, Haas RL, van der Maazen RW. *Role of radiotherapy in the treatment of lymphomas of the gastrointestinal tract. Best Pract Res Clin Gastroenterol.* 2010;24:27-34

Aleman BM, De Bruin ML, Dorresteijn LD, Krol AD, 't Veer MB, Boogerd W, van Leeuwen FE. *Re: Late effects from radiation therapy: the hits just keep on coming. J Natl Cancer Inst* 2010;102:576-577

Al-Mamgani, Heemsbergen WD, Levendag PC, Lebesque JV. *Subgroup analysis of patients with localized prostate cancer treated within the Dutch-randomized dose escalation trial. Radiother Oncol* 2010;96:13-8

Al-Mamgani, Lebesque JV, Heemsbergen WD, Tans L, Kirkels WJ, Levendag PC, Incrocci L. *Controversies in the treatment of high-risk prostate cancer – what is the optimal combination of hormonal therapy and radiotherapy: a review of literature. Prostate* 2010;70:701-09

Annema JT, Bohoslavsky R, Burgers S, Smits M, Taal B, Venmans B, Nabers H, van de Borne B, van Balkom R, Haitjema T, Welling A, Staaks G, Dekkers OM, van Tinteren H, RAbe KF. *Implementation of endoscopic ultrasound for lung cancer staging. Gastrointest Enosc.* 2010;71:64-70

Aukema TS, Rutgers EJ, Vogel WV, Teerstra HJ, Oldenburg HS, Vrancken Peeters MT, Wesseling J, Russell NS, Valdés Olmos RA. *The role of FDG PET/CT in patients with locoregional breast cancer recurrence: A comparison to conventional imaging techniques. Eur J Surg Oncol* 2010;36:387-392

Aukema TS, Straver ME, Vrancken Peeters MT, Russell NS, Gilhuijs KG, Vogel WV, Rutgers EJ, Valdés Olmos RA. *Detection of extra-axillary lymph node involvement with FDG PET/CT in patients with stage III-III breast cancer. Eur J Can* 2010;46:3205-10

Bartelink H, Meijnen P, Straver ME, Rutgers EJ. *The EORTC experience: from DCIS to locally advanced breast cancer. IN: Kuerer's Breast Surgical Oncology. Chapter 45. Kuerer HM, Ed. McGraw-Hill, New York* 2010

## TREATMENT PLANNING

## Including rotations in probabilistic IMRT planning for prostate cancer

Probabilistic planning directly includes geometrical uncertainties during optimization without safety margins, and generally leads to better plans when the PTV overlaps OARs. Our aim was to develop probabilistic planning for marker-based prostate IGRT (where rotations are the main residual uncertainties). Using the prostate's center of mass as rotation point, the effect of random errors is included by blurring the dose distribution for every voxel of the CTV. Next, similar to the Multiple Instance Geometry Approximation, probable CTV instances are calculated for various systematic rotation errors, and then combined with translational errors. Optimization based on a confidence level for a given dose constraint (e.g. DVH point) is achieved by summation over a predefined percentage of lowest cost cases from all systematic errors (typically 90%).

Clinical prostate treatment plans were replanned with probabilistic objectives. Based on a marker-match protocol, uncertainties are largest for systematic rotations around the LR axis (5° SD) and small for translations. Treatment plans from 8 prostate cancer patients were replanned aiming for the same target coverage. Including rotations increased optimization time somewhat (3-5 min). The dose distributions achieved were similar but showed a steeper dose gradient in the rectum region, compensated by an increase in the anterior section of the prostate. Inclusion of rotations led to a dose increase in the seminal vesicle area adjacent to the bladder wall (figure 2). Maintaining the same target coverage, dose to the rectum was reduced by  $5.1 \pm 1.4$  Gy (mean dose). This is the first planning method that correctly includes rotational uncertainties, and inclusion of rotations takes margin-less planning for prostate RT one step closer to clinical implementation.

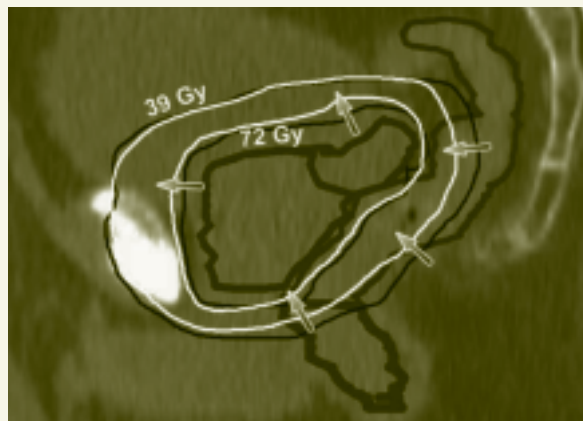


Figure 2: Isodose contours of clinical plan dose (black) and probabilistic plan dose (white) for one of the analyzed patients. Arrows indicate the effect of including rotational uncertainties in optimization

## Sliding eggoid: an accurate algorithm for anisotropic expansion of organs

A recent survey of seven planning systems found a 5% variation of expanded volumes. A sliding ellipsoid does not deal correctly with unequal expansion sizes. The purpose of this work is to develop a fast and accurate expansion algorithm. We propose a sliding 'eggoid': a shape defined by an arbitrary ellipsoid in each octant, with the restriction that the first order derivative of the shape is continuous at the octant borders. The organs are defined as triangulated contours with caps at both ends at half a slice distance. To accelerate the algorithm, only the triangle-edges are sampled, while the original triangles are displaced according to tangent of the triangle to the eggoid. On a normal PC (Intel dual core 3.16 GHz) a 10 mm expansion of a prostate takes 2.1 seconds using a 1.0 mm grid. The accuracy was verified by calculating the volume of an expanded cube and was for all the above grids within 0.5% when a cube of 1.0 cm<sup>3</sup> is anisotropically expanded with eggoids in the range of 10 mm. The novel sliding eggoid algorithm correctly handles anisotropic expansions.

## IMAGE GUIDANCE

**Evaluation of ghosting correction in cone beam CT** Ghosting artifacts reduce image quality and Hounsfield unit accuracy of cone beam CT (CBCT) scans.

Typically, ghosting shows up in transversal planes of CBCT scans as a partial ring with high intensity, and is therefore also referred to as a radar artifact. The

magnitude of ghosting depends on patient and scan geometry and is most apparent when part of the beam is temporarily not attenuated by the patient during gantry rotation. In this study, the image quality improvements of a previously developed correction algorithm were evaluated on CBCT scans of different treatment sites. The parameters for exponential decay were fitted to the falling edge response of a series of cone-beam projection images. To evaluate clinical applicability we reconstructed scans with and without ghosting correction for the treatment sites breast, prostate and liver, manifesting strong, medium and mild ghosting artifacts. Image quality was indeed improved for all reconstructions and the radar artifact was almost completely removed.

**In-vivo analysis of interplay effects due to respiration and respiration irregularities during free-breathing VMAT delivery of SBRT** In free-breathing delivery of lung SBRT with IGRT, the effect of respiratory motion is considered to be a blurring of the dose distribution that can be addressed by small margins. VMAT speeds up dose delivery of SBRT and changes the delivery patterns leading to unknown interplay effects, potentially resulting in unexpected tumor dose heterogeneity. The purpose of this study was to quantify the interplay effect *in-vivo* in individual VMAT patients. We analyzed 5 patients (peak-peak tumor motion 0.2-3 cm, PTV diameter 2.5-6 cm). The analysis uses 3 existing components: 1) The second to second delivered 3D dose is reconstructed using EPID dosimetry software. 2) A motion model of the lung is derived from the 4D planning CT by deformable registration using a phase-based optical flow method. 3) A recording of the respiratory pattern during delivery is obtained by automatic tracking of the diaphragm position in X-rays acquired for 4D CBCT on the linac. When CBCT data is acquired simultaneously with treatment, the interplay effect can be totally quantified *in-vivo* for individual patients. For this analysis, motion traces acquired during separate CBCT acquisitions were used as surrogates. The 4DCT motion model was updated using the diaphragm data as a “navigator channel” to include respiration irregularities. Next, dose reconstructions were deformed according to the instantaneous motion model and accumulated to calculate the actual delivered dose including interplay effects and breathing irregularities. Here we compared the accumulated dose (with interplay effect) with the original 3D EPID dose, and with a simple blurred dose (without interplay effects) according to the motion in the 4D planning CT. With 3 cm motion, the 80% isodose line shifted as expected by about 0.5 cm in the cumulative dose compared to the 3D dose, while there was limited interplay effect: a maximum distance to agreement of 0.3 cm. In other cases, the interplay effect was smaller. In conclusion, we have developed a methodology to analyze interplay effects *in-vivo* in individual patients. The tested VMAT treatments were remarkably robust to the interplay effect and observed respiration irregularities. Therefore, a simple blurring of the 3D dose distribution based on the planning PDF accurately predicts the delivered dose.

## ADAPTIVE RADIOTHERAPY

### Plan adaptation for systematic deformations in head & neck cancer radiotherapy based on an average patient model

A new CT is commonly acquired to adapt to progressive anatomy changes (e.g. weight loss) during radiotherapy for H&N cancer patients. However, both the planning and the repeat CT are snapshots of a variable patient pose and thus introduce systematic deformations. The purpose of this study was to validate the application of an average patient model obtained by the modification of the planning CT. Displacement Vector fields (DVF) for 10 patients were obtained by B-spline deformable registration between the planning CT and daily CBCTs ( $\pm$  31 fractions per patient). We compared the following protocols: online couch shifts (as reference), single plan adaptation with one <DVF> after N scans, and weekly adaptation based on an <DVF> from the previous week. We calculated the average vector length (over all patients) of the average displacement vector (over all fractions) of bony (B) and soft tissue (ST) landmarks. Effectiveness of single plan adaptation depended on the number of measurements, with an optimum at 12, though the overall effectiveness was modest (B: 1.5 mm, ST: 2.9 mm), indicating progressive changes. Weekly plan adaptation showed a higher accuracy of (B: 1.2 mm, ST: 2.1 mm) as it performs

## Publications (continued)

Beekman CA, Buckle T, van Leeuwen AC, Valdés Olmos RA, Verheij M, Rottenberg S, van Leeuwen FW. *Questioning the value of (99m)Tc-HYNIC-annexin V based response monitoring after docetaxel treatment in a mouse model for hereditary breast cancer. Appl Radiat Isot. 2010 (in press)*

Bex A, Sonke GS, Pos FJ, Brandsma D, Kerst JM, Horenblas S. *Symptomatic brain metastases from small-cell carcinoma of the urinary bladder: The Netherlands Cancer Institute experience and literature review. Ann Oncol 2010;11:2240-5*

Borst GR, Sonke JJ, Belderbos JS, Lebesque JV. *Normal tissue complication probability after hypofractionation increased due to the high dose per fraction or the high total biological equivalent dose? Radiother Oncol 2010;94:388*

Borst GR, Ishikawa M, Nijkamp J, Hauptmann M, Shirato H, Bengua G, Onimaru R, Josien Bois AD, Lebesque JV, Sonke JJ. *Radiation pneumonitis after hypofractionated radiotherapy; evaluation of the LQ (L) model and different dose parameters. Int J Radiat Oncol Biol Phys 2010;77:1596-603*

Borst GR, Sonke JJ, Hollander SD, Betgen A, Remeijer P, van Giersbergen A, Russell NS, Elkhuizen PH, Bartelink H, van Vliet-Vroegindewij C. *Clinical results of Image-Guided Deep Inspiration Breath Hold Breast Irradiation. Int J Radiat Oncol Biol Phys 2010;78:1346-51*

Broeks A, Braaf LM, Wessels LF, van de Vijver M, de Bruin ML, Stovall M, Russell NS, van Leeuwen FE, van 't Veer LJ. *Radiation-associated breast tumors display a distinct gene expression profile. Int J Radiat Oncol Biol Phys 2010;76:504-7*

Burke SM, van de Giessen E, de Win M, Schilt T, van Herk M, van den Brink W, Booij J. *Serotonin and dopamine transporters in relation to neuropsychological functioning, personality traits and mood in young adult healthy subjects. Psychol Med 2010;6:1-11*

Case RB, Moseley DJ, Sonke JJ, Eccles CL, Dinniwell RE, Kim J, Bezjak A, Milosevic M, Brock KK, Dawson LA. *Interfraction and intrafraction changes in amplitude of breathing motion in stereotactic liver radiotherapy. Int J Radiat Oncol Biol Phys 2010;77:918-925*

## Publications (continued)

Chai X, van Herk M, van de Kamer JB, Remeijer P, Bex A, Betgen A, De Reijke TM, Hulshof MC, Pos FJ, Bel A. *Behavior of Lipiodol Markers During Image Guided Radiotherapy of Bladder Cancer. Int J Radiat Oncol Biol Phys* 2010;77:309-14

Courrech Staal EF, Aleman BM, Boot H, van Velthuysen MF, van Tinteren H, van Sandick JW. *Systematic review of the benefits and risks of neoadjuvant chemoradiation for oesophageal cancer. British J of Surg* 2010;97:1482-96

Courrech Staal EF, Aleman BM, van Velthuysen ML, Cats A, Boot H, Jansen EP, van Coevorden F, van Sandick JW. *Chemoradiation for esophageal cancer: Institutional experience with three different regimens. Am J Clin Oncol* 2010 (in press)

de Jong MC, Pramana J, Kneijens JL, Balm AJ, van den Brekel MW, Hauptmann M, Begg AC, Rasch CR. *HPV and high-risk gene expression profiles predict response to chemoradiotherapy in head and neck cancer, independent of clinical factors. Radiother Oncol* 2010;95:365-70

de Jong MC, Pramana J, van der Wal JE, Lacko M, Peutz-Kootstra CJ, de Jong JM, Takes RP, Kaanders JH, van der Laan BF, Wachters J, Jansen JC, Rasch CR, van Velthuysen ML, Grenman RA, Hoebbers FJ, Schuurung E, van den Brekel MW, Begg AC. *CD44 expression predicts local recurrence after radiotherapy in larynx cancer. Clin Cancer Res* 2010;16:5329-38

de Vreeze R, de Jong D, Nederlof P, Ruijter HJ, Boerrigter L, Haas R, van Coevorden F. *Multifocal myxoid liposarcoma-metastasis or second primary tumor?: a molecular biological analysis. J Mol Diagn* 2010;12:238-43

de Vreeze RS, de Jong D, Nederlof PM, Ariaens A, Tielen IH, Frenken L, Haas RL, van Coevorden F. *Added value of molecular biological analysis in diagnosis and clinical management of liposarcoma: A 30-Year single-institution experience. Ann. Surg Oncol* 2010;17:683-93

de Vreeze RS, de Jong D, Koops W, Nederlof PM, Ariaens, Haas RL, van Coevorden R. *Oncogenesis and classification of mixed-type liposarcoma: a radiological, histopathological and molecular biological analysis. Int J Cancer* 2010 (in press)

better on progressive changes. For patients with overall systematic deformations  $\geq 3$ mm, weekly adaptation reduced systematic deformations by more than 45%. Inability of the deformable registration method to register sliding tissue (tip of uvula and epiglottis occasionally led to large systematic ST errors. We conclude that the benefits of this method are potentially high for patients with large deformations.

## FOLLOW-UP RESEARCH

**Post chemoradiation FDG-PET derived local radiation dose effect relation for oesophageal toxicity in NSCLC patients** Non Small Cell Lung Cancer (NSCLC) patients undergoing concurrent chemoradiation (CRT) using IMRT in our institute, often develop severe acute radiation oesophagitis. The purpose of this work was to correlate the planned dose distribution with the post-CRT local oesophageal FDG-PET uptake as a surrogate for oesophageal toxicity to improve our understanding of the dose effect relationship. Ten NSCLC patients (2 groups: 5 patients with grade 1-2, and 5 patients with grade 3 oesophageal toxicity) partaking in a phase II combined modality treatment study (concurrent chemoradiation with cetuximab) were selected from a total of 43 study patients. Patients were selected where the oesophagus was within the planning target volume (PTV) and an FDG-PET/CT scan was performed approximately 30 days post-CRT. IMRT was combined with daily cisplatin and weekly cetuximab. The planned dose was sampled on the oesophagus surface. The post-CRT-PET scan was recalculated to standard uptake values (SUV) and sampled on the oesophagus surface to establish the oesophageal dose to FDG-PET SUV relationship. The mean PET SUV for the oesophagus surface was significantly higher in the grade 3 oesophageal toxicity group compared to the grade 1-2 group (2.7 vs. 2.1,  $p=0.04$  1-sided t-test). A local dose-effect relationship was observed with a sharp increase in average oesophageal FDG-PET activity at dose levels above 60 Gy. At these high dose levels significant differences in planned oesophageal dose were present between patients with grade 1-2 and grade 3 toxicity. The results indicate that elevated SUV post-CRT in the oesophagus is correlated with severe acute oesophageal toxicity and that local FDG-PET uptake values mostly increase at EQD2 levels above 60 Gy. These observations indicate that the previously used predictor  $V_{35}$  may not be accurate for oesophagus toxicity after IMRT (figure 3).

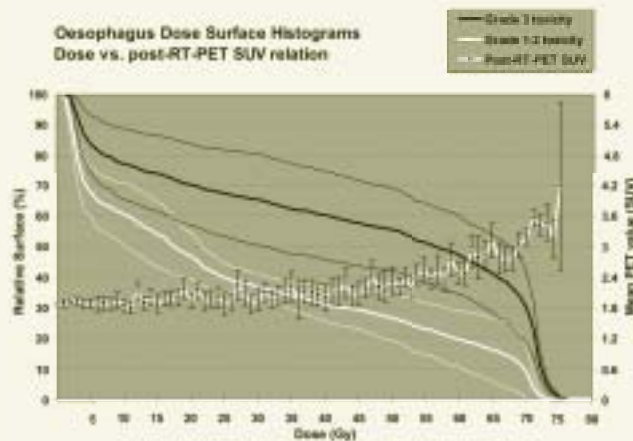


Figure 3: Average relative oesophagus dose-surface histogram for patients with grade 3 toxicity (thick black) and patients with grade 1-2 toxicity (thick white) and their 95% CI (thin lines). The line with square markers denotes the relationship between planned dose at the surface of the oesophagus and the PET Standard Uptake Value measured at that same point post-RT, error bars are 95% CI.

## Use of principal component analysis to analyze inter-patient dose variation

Dose variation between prostate cancer patients is the result of a limited number of factors, such as local differences in the shape, position and volume prostate and seminal vesicles. The purpose of this study is to analyze the inter-patient dose variation using principal component analysis (PCA), in relation to outcome. A subgroup of 67 patients with localized prostate cancer and a high risk for extraprostatic disease was selected from the Dutch trial. Failure ( $n=30$ ) was biochemical or clinical determined at a 4 year endpoint. For each patient a 3-dimensional dose map was created around the prostate, on a fixed grid of dose points. Afterwards, we applied PCA to obtain the uncorrelated principal components (PCs). Every PC represents a weighted linear combination of dose voxels. Pearson correlation coefficients were then computed between these PCs and several factors.

## Publications (continued)

Dikken JL, Jansen EP, Cats A, Bakker B, Hartgrink HH, Kranenbarg EM, Boot H, Putter H, Peeters KC, van de Velde CJ, Verheij M. Reply to F. Scalfani et al. *J Clin Oncol*. 2010

Dikken JL, Jansen EP, Cats A, Bakker B, Hartgrink HH, Meershoek-Klein Kranenbarg E, Boot H, Putter H, Peeters KC, van de Velde CJ, Verheij M. Impact of the extent of surgery and postoperative chemoradiotherapy on recurrence patterns in gastric cancer. *J Clin Oncol* 2010;28:2430-6

Elshof LE, Rutgers EJ, Deurloo EE, Loo CE, Wesseling J, Pongel KE, Gilhuijs KG. A practical approach to manage additional lesions at preoperative breast MRI in patients eligible for breast conserving therapy: results. *Breast Canc Res Treat* 2010;124:717-21

Fuller CD, Nijkamp J, Duppen JC, Rasch CR, Thomas JR Jr, Wang SJ, Okunieff P, Jones WE 3<sup>rd</sup>, Baseman D, Patel S, Demandante CG, Harris AM, Smith BD, Katz AW, McGann C, Harper JL, Chang DT, Smalley S, Marshall DT, Goodman KA, Papanikolaou N, Kachnic LA. Prospective randomized double-blind pilot study of site-specific consensus atlas implementation for rectal cancer target volume delineation in the cooperative group setting. *Int J Radiat Oncol Biol Phys* 2010;79:481-9

Graafland NM, van Boven HH, van Werkhoven E, Moonen LM, Horenblas S. Prognostic significance of extranodal extension in patients with pathological node positive penile carcinoma. *J Urol* 2010;184:1347-53

Heemsbergen WD, Al-Mamgani A, Witte MG, van Herk M, Pos FJ, Lebesque JV. Urinary obstruction in prostate cancer patients from the Dutch trial (68 Gy vs. 78 Gy): Relationships with local dose, acute effects, and baseline characteristics. *Int J Radiat Oncol Biol Phys* 2010;78:19-25

Hoving S, Heeneman S, Gijbels MJ, te Poele JA, Bolla M, Pol JF, Simons MY, Russell NS, Daemen MJ, Stewart FA. NO-donating aspirin and aspirin partially inhibit age-related atherosclerosis but not radiation-induced atherosclerosis in ApoE null mice. *PLoS One*. 2010;5:e12874

Finally, the logistic regression model was used to evaluate the predicted value of the PCs on failure. The first three PCs explain the most variation (37.5%, 15.4% and 7.6%). All three PCs appear to correlate with the length of the delineated seminal vesicles in LR, CC or AP directions: PC1 mainly correlates with CC direction ( $R=0.65$ ,  $P<0.001$ ), PC2 with LR direction ( $R=0.57$ ,  $P<0.001$ ), and PC3 also with CC direction ( $R=0.52$ ,  $P<0.001$ ). The rotation and the volume of the seminal vesicles correlate with PC1 ( $R=-0.85$ ,  $P<0.001$ ) and PC2 ( $R=0.42$ ,  $P<0.001$ ), respectively. The volume of the prostate correlates with PC3 ( $R=0.57$ ,  $P<0.001$ ). When we applied forward logistic regression on all three PCs, only PC2 ( $P=0.005$ ) was shown to be as a significant predictor, while PC1 and PC3 ( $P>0.2$ ) are not. In conclusion, PCA identified an uncorrelated dose component (PC2) that is significantly associated with the outcome. Furthermore, the length in LR direction and the volume of the seminal vesicles are correlated with this component.

### Radiotherapy in high-risk prostate cancer: randomization to rectangular fields associated with less early clinical failures compared to the conformal arm

In a prior investigation as well as the above-mentioned PCA study we concluded that incidental dose in nodal areas was associated with failure in high risk prostate cancer patients treated to the prostate and seminal vesicles (SV) only. Data of another study were available to validate our assumptions. In a first analysis, we investigated whether rectangular fields were associated with less early clinical failures than conformal fields for these patients. From a trial population of 266 T1-T4N0M0 patients, we selected 172 high-risk patients with localized prostate cancer (PSA > 20  $\mu\text{g/L}$ , or poor differentiation, or T3) who had been randomized between rectangular ( $n=83$ ) and conformal fields ( $n=88$ ). The prescribed dose was 66 Gy with 15 mm margin. Main trial objective was to compare toxicity, but data on clinical failure were also available for all trial patients. Median follow-up was 32 months (range 2-48). The Number of events in the high-risk group was 12 in the rectangular arm and 26 in the conformal arm. Kaplan Meier estimates showed a significant lower risk of clinical failure for rectangular fields ( $p=0.02$ , figure 4) compared to conformal fields. We evaluated at which anatomical locations more dose was delivered outside the prostate, for the rectangular vs. conformal fields. We found dose differences in the range of 5-35 Gy between the arms in the obturatorial and presacral nodal areas, which is indicated in figure 4 below: we plotted iso dose difference lines (5,15,25 Gy) on a sagittal and coronal CT view of a sample patient. We conclude that early clinical failures can possibly be prevented by elective nodal irradiation for high-risk prostate cancer patients.



Figure 4: Kaplan Meier for clinical failure (left), and coronal (middle) plus sagittal (right) view with iso dose difference lines (mean, Gy), indicating the regions where the rectangular arm patients received on average more dose compared to the conformal arm.

### 3D analysis of recurrence patterns in rectal cancer and its consequences for the clinical target volume in hypo-fractionated preoperative radiotherapy

For preoperative RT of rectal cancer the clinical target volume (CTV) is very much dependent of the cranio-caudal level of the tumor, while nodal status and expected circumferential resection margin (CRM) hardly have influence. CRM and nodal status are, however, predictive for local recurrences, and with MR they can be estimated in advance. The aim of this study was to determine whether and where the CTV can be adapted based on the nodal status and CRM parameters. Patients

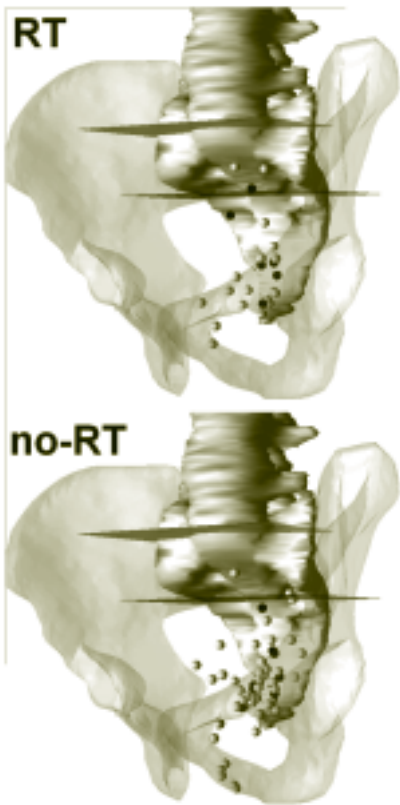


Figure 5: Locations of the local recurrences in the RT (top) and no-RT (bottom) group colored for NO and CRM – (black dots and N+ and /or CRM+ (white dots) Top plane indicates the cranial border of the used RT fields, while the bottom plane indicates the S2 - S3 inter - space level.

treated in the Dutch total mesorectal excision (TME) trial, either with a TME alone (no-RT) or with 5x5 Gy RT followed by a TME (RT), with a local recurrence were analyzed. A local recurrence was found in 114 of 1417 patients in the trial. For 94 (25 RT; 69 no-RT) recurrences the location was adequately known to be placed in a 3D pelvic model. The influence of preoperative RT on patterns of local recurrence was evaluated. The use of RT mainly reduces anastomotic, lateral and perineal recurrences. In patients with No disease and a negative CRM only one recurrence was found cranially of the S2-S3 inter-space (figure 5). This was for an RT patient and only 2 lymph nodes were examined during pathology. A reduction of the CTV border cranially to the S2-S3 inter-space is proposed which would lower the cranial border by approximately 4 cm while a maximum increase in local recurrence rate of 0.2% can be expected. With the proposed CTV, a reduction in absolute small bowel exposure (>15 Gy) of approximately 40% and 60% could be achieved for 3-field conformal- and IMRT, respectively.

**PRECLINICAL IMAGING**

**Performance characterization of a high-resolution imaging system for small animal radiation research**  $\mu$ IGRT systems bridge the technology gap between pre-clinical radiation research and clinical radiation therapy by combining a high accuracy CBCT imaging system and a high dose therapeutic X-ray source on the same platform. The purpose of this research was to quantify the CBCT image quality improvements of a new flat panel imager (FPI).

We evaluated  $\mu$ IGRT systems: Unit 1 contains a FPI with a Gd<sub>2</sub>O<sub>3</sub> scintillator and a pixel pitch of 400  $\mu$ m (512x512 pixels), Unit 2 contains a FPI with a CsI scintillator and a 200  $\mu$ m pixel pitch (1024x1024 pixels). Image uniformity, system spatial resolution and contrast to noise ratio (CNR) were studied on a  $\mu$ CT image quality phantom.

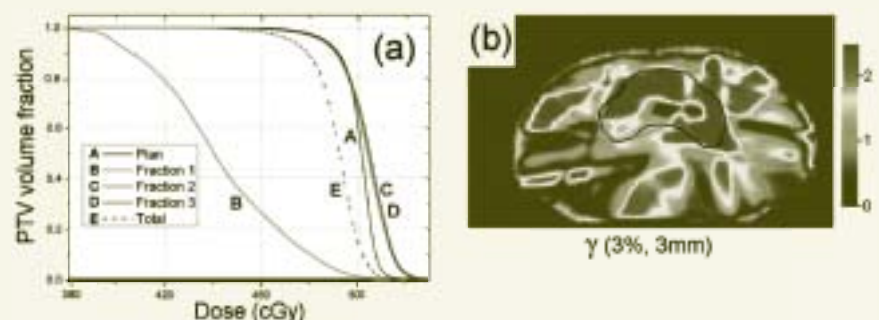
The full width at half maximum of the modulated transfer function (MTF) increased from 0.7 mm<sup>-1</sup> of unit 1 to 2.1 mm<sup>-1</sup> for unit 2. The MTF value at 10% of the maximum indicates that structures of 200  $\mu$ m can be resolved with Unit 2. CNR was about 30% lower in unit 2 for the same voxel size. Image uniformity was similar between the two units with variations of about 4%.

**EPID DOSIMETRY**

Priscilla Camargo, Anton Mans, Igor Olaciregui-Ruiz, Raul Pecharromán-Gallego, Jan-Jakob Sonke, Joep Stroom, Marcel van Herk, Ben Mijnheer

The potential for incidents and the ever-increasing complexity of patient treatments emphasize the need for accurate dosimetric verification in radiotherapy. For this reason, all curative treatments are verified by EPID (Electronic Portal Imaging Device) dosimetry. Since the clinical introduction of the method in February 2005 treatment plans of more than 5000 patients have been verified. The results of these measurements have recently been analyzed. Among these plans, 17 serious errors were detected that have led to an intervention. Due to their origin, 9 of these errors would not have been detected with pre-treatment verification, including a plan transfer error detected in a 5x5 Gy IMRT rectum treatment (see figure 6). Investigation of the plan transfer chain revealed that due to a network transfer error (“lost delayed write data”) the plan was corrupted. 3D analysis of the acquired EPID data revealed serious under-dosage of the PTV: on average 11.6%, locally up to 20%. The information was used by the physician to determine whether and to what extent

Figure 6: a) PTV DVHs from planned dose distribution ('A'), EPID reconstructed dose distributions of fractions 1-3 ('B'-'D') and total EPID reconstructed dose distribution (fractions 1-5) ('E'). (b) Axial plane from a 3D -evaluation of the first fraction, intersecting the isocenter; the PTV is indicated.



## Publications (continued)

Jansen EP, Boot H, Dubbelman R, Verheij M, Cats A. *Postoperative chemoradiotherapy in gastric cancer – a phase I-II study of radiotherapy with dose escalation of weekly cisplatin and daily capecitabine chemotherapy.* *Ann Oncol.* 2010;21:530-4

Jansen EPM, Nijkamp J, Gubanski M, Lind PARM, Verheij M. *Interobserver variation of clinical target volume delineation in gastric cancer.* *Int J Radiat Oncol Biol Phys* 2010;77:1166-70

Kappers I, van Sandick JW, Burgers SA, Belderbos JS, van ZN, Klomp HM. *Surgery after induction chemotherapy in stage IIIA-N2 non-small cell lung cancer: Why pneumonectomy should be avoided.* *Lung Cancer* 2010;68:222-7

Knauer M, Mook S, Rutgers EJ, Bender RA, Hauptmann M, van de Vijver MJ, Koorstra RH, Bueno-de-Mesquita JM, Linn SC, van 't Veer LJ. *The predictive value of the 70-gene signature for adjuvant chemotherapy in early breast cancer.* *Breast Cancer Res Treat* 2010;120:655-61

Knegjens JL, Hauptmann M, Pameijer FA, Balm AJ, Hoebbers FJ, de Bois JA, Kaanders JH et al. *Tumor volume as prognostic factor in chemoradiation for advanced head and neck cancer.* *Head & Neck*, 2010;1-9

Kreike B, Hart G, Bartelink H, van de Vijver MJ. *Analysis of breast cancer related gene expression using natural splines and the Cox proportional hazard model to identify prognostic associations.* *Breast Cancer Res Treat* 2010;122:711-20

Le C, van de Weijer EP, Pos FJ, Vogel WV. *Active inflammation in 18F-methylcholine PET/CT.* *Eur J Nucl Med Mol Imaging* 2010;37:654-655

Mann RM, Loo CE, Wobbes T, Bult P, Barentsz JO, Gilhuijs KGA, Boetes C. *The impact of preoperative breast MRI on the re-excision rate in invasive lobular carcinoma of the breast.* *Breast Cancer Res Treat* 2010;119:415-422

Mans A, Remeijer P, Olaciregui-Ruiz I, Wendling M, Sonke JJ, Mijnheer B, van Herk M, Stroom JC. *3D Dosimetric verification of volumetric-modulated arc therapy by portal dosimetry.* *Radiother Oncol.* 2010;94:181-7

compensatory measures were needed in the remaining four fractions. This analysis shows the importance of *in vivo* (EPID) dosimetry for all treatment plans as well as the ability of our method to assess the dosimetric impact of deviations found.

Volumetric-modulated arc therapy (VMAT) of prostate and lung cancer has been introduced in our department in 2009. VMAT is a complex technique in which gantry speed, field shape and dose rate are continuously varied during gantry rotation. Consequently, accurate verification is essential for a safe clinical implementation of VMAT. EPID images obtained during VMAT delivery using gantry-angle resolved data acquisition are converted to 3D dose distributions inside a phantom or patient using our back-projection model. In addition to verification of the dose at the isocentre, 3D gamma analysis is performed to compare planned and EPID-reconstructed 3D VMAT dose distributions. Gamma evaluation parameters are mean and maximum (1%) gamma and % gamma < 1. VMAT plans of 10 prostate and 10 lung cancer patients, verified by means of 3D EPID dosimetry, have been analysed. The average difference of the dose at the isocentre was for prostate cancer VMAT  $-0.2 \pm 1.6$  % and  $+0.4 \pm 1.6$  %, pre-treatment and *in vivo*, respectively, and for the hypo-fractionated lung cancer VMAT plans  $+2.0 \pm 1.2$  % and  $-0.7 \pm 2.3$  %. 3D gamma evaluation showed almost the same results for pre-treatment and *in vivo* verification of the 3D dose distribution for prostate cancer VMAT, while somewhat larger deviations were observed for lung cancer VMAT verification. The results of this study show that EPID dosimetry is a valuable tool for 3D verification of VMAT delivery, both pre-treatment and *in vivo*.

Currently the transmission of the photon beam through a phantom or patient, an essential ingredient of the back-projection model, is estimated from the ratio of EPID measurements with and without a phantom/patient in the beam. Thus, an additional irradiation to obtain “open images” under the same conditions as the actual phantom/patient irradiation is required. However, by calculating the transmission in the direction of the beam instead of using “open images”, this extra measurement can be avoided. This was achieved by using a model that includes the effect of beam hardening and off-axis dependence of the EPID response. The parameters in the model were empirically obtained by performing EPID measurements using polystyrene slab phantoms of different thickness. A theoretical analysis to verify the sensitivity of the model with patient thickness changes was also performed. The new model was applied for EPID dose verification measurements of various IMRT treatments. The results showed generally good agreement with the dose determined using the measured transmission. The average difference between EPID-based *in vivo* dose at the isocentre determined using either the new model for transmission or its measured value, was  $2.6 \pm 3.1$ ,  $0.2 \pm 3.1$  and  $2.2 \pm 3.9$  %, for 47 patients treated with 6, 10 and 18 MV IMRT beams, respectively. For a sub-group of 11 patients pre-treatment verification was also performed showing similar dose differences at the isocentre:  $-1.9 \pm 0.9$ ,  $-1.4 \pm 1.2$  and  $-0.4 \pm 2.4$  %. It can be concluded that calculating instead of measuring the transmission leads to differences in dose generally smaller than 2 % and yielded only slightly higher gamma evaluation parameter values. The new model is now tested clinically for a large variety of treatment sites.

Our current EPID-based back-projection dose reconstruction model had to be modified to make it also applicable to wedged beams. For this purpose an energy-dependent correction factor, taking into account the changes in beam quality caused by the wedge and the presence of a phantom or patient, was inserted in the EPID dose-response function. The resulting reconstructed dose distribution was in good agreement with the planned dose in a plane at 10 cm depth in a patient but does not take the depth dependence of the wedge factor into account. A start has been made to extend the wedge correction model for 3D dose verification of wedged beams.

## TREATMENT PLANNING

Corine van Vliet-Vroegindeweij, Andrea Holt, Tomas Janssen, Zdenko van Kesteren, Emmy Lamers, Annemarie Lakeman, Angela Tjihuis, Suzanne den Hollander, Anton Mans, Anke van Mourik, Roman Bohoslavsky, Marnix Witte, José Belderbos, Coen Rasch, Joost Knegjens, Jan-Jakob Sonke, Paula Elkhuizen, Tanja Alderliesten, Jonathan Yang, Eugène Damen

## Publications (continued)

Mans A, Wendling M, McDermott LN, Sonke JJ, Tielenburg R, Vijlbrief R, Mijnheer B, van Herk M, Stroom JC. *Catching errors with in vivo EPID dosimetry. Med Phys* 2010;37:2638-44

Matzinger O, Heimsoth I, Poortmans P, Collette L, Struikmans H, Van Den Bogaert W, Fourquet A, Bartelink H, Ataman F, Gulyban A, Pierart M, Van Tienhoven G; EORTC Radiation Oncology & Breast Cancer Groups. *Toxicity at three years with and without irradiation of the internal mammary and medial supraclavicular lymph node chain in stage I to III breast cancer (EORTC trial 22922/10925). Acta Oncol* 2010;49:24-34

Mook S, Knauer M, Bueno-de-Mesquita JM, Retel VP, Wesselink J, Linn SC, van 't Veer LJ, Rutgers EJ. *Metastatic Potential of T1 Breast Cancer can be predicted by the 70-gene MammaPrint Signature. Ann Surg Oncol* 2010;17:1406-13

Mook S, Schmidt MK, Weigelt B, Kreike B, Eekhout I, van de Vijver MJ, Glas AM, Floore A, Rutgers EK, van 't Veer LJ. *The 70-gene prognosis signature predicts early metastasis in breast cancer patients between 55 and 70 years of age. Ann Surg Oncol* 2010;21:717-22

Nijkamp J, Kusters M, Beets-Tan RGH, Martijn H, Beets GL, Van de Velde CJH, Marijnen CAM. *Three-dimensional analysis of recurrence patterns in rectal cancer: The cranial border in hypofractionated preoperative radiotherapy can be lowered. Int J Radiat Oncol Biol Phys* 2010 (in press)

Okines A, Verheij M, Allum W, Cunningham D & Cervantes A on behalf of the ESMO guidelines working group. *Gastric cancer: ESMO clinical practice guidelines for diagnosis, treatment and follow-up. Annals of Oncol* 2010;21:50-54

Oldenburg S, Van Os RM, Van Rij CM, Crezee J, Van de Kamer JB, Rutgers EJ, Geijsen ED, Zum vörde sive vörding PJ, Koning CC, Van Tienhoven G. *Elective re-irradiation and hyperthermia following resection of persistent locoregional recurrent breast cancer: A retrospective study. Int J Hyperthermia* 2010;26:136-44

Pos F, Remeijer P. *Adaptive management of bladder cancer radiotherapy. Semin Radiat Oncol* 2010;20:116-120

### Biological Target Volume (BTV) boost phase II study on dose-escalation of the high uptake FDG-PET regions inside the primary tumor for NSCLC

Recurrences in NSCLC occur mainly in the high FDG uptake regions visible on the pre-treatment CT-PET scan. Dose-escalation of these high FDG uptake regions might improve local control and overall survival. In cooperation with Maastric clinic, we therefore designed a randomized phase II trial with 2 treatment arms: dose-escalation up to the normal tissue constraints using a simultaneous integrated boost (SIB) to the entire primary tumour (Arm A) or to the regions inside the primary tumour having an FDG-uptake  $\geq 50\%$  of maximum SUV (Arm B). A treatment planning study was performed on 7 patients to investigate the feasibility of this trial design. Current clinical plans deliver a dose of 66 Gy in 24 fractions to the primary tumor. Dose-escalation is planned as a SIB up to a maximum fraction dose of 5.5 Gy based on the normal tissue constraints; e.g. mediastinal structures: max. 94 Gy, brachial plexus: max. 66 Gy, lungs: MLD 20 Gy, spinal cord: max. 52 Gy, all doses in EQD<sub>2</sub>.

In 2 patients the brachial plexus restricted dose-escalation, and for 2 patients the acceptable lung toxicity was reached already at the conventional dose level of 66 Gy due to the large volume of the PTV. For 3 patients, the dose-escalation was planned for both treatment arms. Mean dose-escalation levels for the entire PTV (Arm A) were up to 73 Gy, 74 Gy and 101 Gy, whereas higher levels of dose-escalation were obtained in Arm B: 76 Gy, 77 Gy and 134 Gy, respectively. The normal tissues limiting further dose-escalation were lung (N=2) and the mediastinal structures (N=3). For one patient in Arm B, the tumour dose reached the maximum allowed dose-escalation.

Based on these results, we conclude that dose-escalation using a SIB to the high FDG uptake regions or the entire primary tumour is feasible. Because of the size of the primary tumour in stage II/III NSCLC, dose-escalation is frequently restricted by the normal mediastinal structures (blood vessels), mean lung dose and the brachial plexus.

The first patient entered the phase II randomized trial in May 2010 and 9 patients have been entered so far.

### VMAT for stereotactic body radiation therapy of lung tumors: a comparison with conventional IMRT techniques

For a random selection of 27 patients eligible for SBRT, we generated treatment plans for three different treatment techniques: 1. a coplanar VMAT technique (using the SmartArc module in Pinnacle<sup>3</sup>), 2. our clinically used non-coplanar IMRT technique including typically 12-16 non-coplanar beams, and 3) a coplanar IMRT technique including 9 equidistant beams. A dose of 3x18 Gy was prescribed to the isodose encompassing 95% of the PTV. The dose to healthy lung tissue was judged using the biologically equivalent dose in fractions of 2 Gy (EQD<sub>2</sub>) using the linear-quadratic model with  $\alpha/\beta = 3$  Gy and should not exceed 16 Gy. The maximum dose for OAR's should be below physical doses of 18 Gy for the spinal cord, 30 Gy for the heart, 27 Gy for the esophagus, and 24 Gy for the brachial plexus.

Clinically acceptable VMAT plans could be prepared using two coplanar arcs, where radiation entering through the contralateral lung was avoided. Treatment delivery times for VMAT could be reduced to an average of 6.6 minutes as compared to 23.7 minutes for non-coplanar IMRT. The mean dose to healthy lung in EQD<sub>2</sub> was found to be very similar for VMAT (8.5 Gy) and non-coplanar IMRT (8.4 Gy), and slightly increased for coplanar IMRT (8.9 Gy). The dose conformity of the 54 Gy isodose level was 1.13 for VMAT and 1.11 for non-coplanar IMRT and 1.12 for coplanar IMRT. For the lower isodose levels the conformity was found to be slightly better for non-coplanar IMRT with 4.8 vs. 5.2 for VMAT at the 27 Gy isodose level. Sparing of OAR's including spinal cord, esophagus, heart, brachial plexus and large blood vessels can be achieved with VMAT at levels comparable to and sometimes even better than with non-coplanar IMRT.

We concluded that coplanar VMAT for SBRT of early-stage lung cancer achieved a plan quality and sparing of OAR's comparable to non-coplanar IMRT and slightly better to that of coplanar IMRT, while delivery time can be reduced by up to 70% with VMAT. Based on these results, VMAT for SBRT of lung cancer has been successfully implemented in our clinic.

**Sequentially delivered boost plans are superior to simultaneously delivered plans in head-and-neck cancer when the boost volume is located further away from the parotid glands** We evaluated 50 recently treated head and neck cancer patients. Apart from the clinical plan with a sequentially (SEQ) given boost using an IMRT technique, a simultaneous integrated boost (SIB) technique plan was constructed with the same beam set-up. The mean dose to the parotid glands was compared. The elective nodal areas were bilateral in all cases, with a boost on either one side or both sides of the neck.

When the parotid gland volume and the Planning Target Volume (PTV) for the boost overlap, there is on average a lower dose to the parotid gland with a SIB technique (-1.2 Gy) which is however not significant ( $p=0.08$ ). For all parotid glands with no boost PTV overlap, there is a benefit from a SEQ technique compared to a SIB technique for the gland evaluated (on average a 2.5 Gy lower dose to the parotid gland,  $p<0.001$ ). When the distance between gland and PTV is 0-1 cm, this difference is on average 0.8 Gy, for 1-2 cm distance 2.9 Gy and for glands with a distance greater than 2 cm, 3.3 Gy. When the lymph nodes on the evaluated side are also included in the boost PTV, however, this relationship between the distance and the gain of a SEQ seems less clear.

We concluded that a sequentially delivered boost technique results in a better treatment plan for most cases, compared to a simultaneous integrated boost IMRT technique, if the boost PTV is more than 1 cm away from at least one parotid gland.

**Inter-institutional collaboration for the clinical introduction of VMAT for head-and-neck cancer** In the Netherlands, five institutes established a workgroup to aid a fast and secure clinical introduction of VMAT for treatment of head-and-neck cancer (HNC) and to assure a high quality of VMAT treatment planning in all participating institutes. CT datasets of five patients including delineated structures were shared. Four institutes used Pinnacle<sup>3</sup> (Philips Medical Systems) and one institute Oncentra Masterplan (Nucletron) to produce treatment plans to be delivered on Elekta linear accelerators equipped with a standard MLC or a beam modulator. According to a treatment protocol agreed on beforehand by all participating institutes, which included a guideline for dose prescription and plan acceptance criteria, VMAT and IMRT plans were generated for a simultaneous integrated boost (SIB) treatment of HNC.

All institutes rapidly succeeded in producing clinically acceptable VMAT plans with only small changes to the inverse planning objectives used for IMRT. Differences between both IMRT and VMAT plans of different institutes tended to be small, and may be due to the planner's preferences, guided by each institute's clinical practice. Discussion of the results and exchange of information regarding VMAT treatment planning parameters and objectives resulted immediately in further improvement of the VMAT plans. Preliminary results from comparison of VMAT and IMRT plans of the same institute for a single patient showed significantly better sparing for most OAR's. In this case, the mean dose to parotids and oral cavity was reduced to on average 23 Gy and 33 Gy for VMAT, respectively, as compared to 25 Gy and 35.5 Gy for IMRT. VMAT plans were found to have an overall better conformity for the elective PTV. All institutes reported for VMAT a reduction in delivery times with about 50% as compared to IMRT.

Collaboration between institutes on the clinical introduction of a new treatment modality can help to accelerate the learning curve and, resulting from exchange and discussion within the group, to achieve a high quality of treatment planning within a short time. VMAT plans for SIB treatments of HNC were found to be comparable or better than IMRT plans, while delivery time can be significantly shortened.

**A radiotherapy replanning guideline for patients who develop seroma after breast-conserving surgery** For breast cancer patients who develop seroma in the excision cavity after breast-conserving surgery (BCS) the seroma is often used for delineating the boost volume. However, seroma reduction of 54% during radiotherapy (RT) has been reported. We investigated which guidelines for monitoring and replanning breast patients with seroma are safe for clinical implementation. Twenty-one patients who developed seroma after BCS were included. For each patient a pre-treatment CT (CT<sub>1</sub>), a CT in the third (CT<sub>3</sub>) and a CT in the fifth week

Rasch CR, Steenbakkers RJ, Fitton I, Duppen JC, Nowak PJ, Pameijer FA, Eisbruch A, Kaanders JH, Paulsen F, van Herk M. *Decreased 3D observer variation with matched CT-MRI, for target delineation in nasopharynx cancer. Radiat Oncol* 2010;5:21

Rasch CR, Hauptmann M, Schornagel J, Wijers O, Buter J, Gregor T, Wiggenraad R, Paul de Boer J, Ackerstaff AH, Kroger R, Hoebbers FJ, Balm AJ. *Intra-arterial versus intravenous chemoradiation for advanced head and neck cancer: Results of a randomized phase 3 trial. Cancer* 2010;116:2159-65

Schmitz AC, van den Bosch MA, Loo CE, Mali WP, Bartelink H, Gertenbach M, Holland R, Peterse JL, Rutgers EJ, Gilhuijs KG. *Precise correlation between MRI and histopathology – exploring treatment margins for MRI-guided localized breast cancer therapy. Rad and Onc* 2010;97:225-32

Smitsmans MH, de Bois J, Sonke JJ, Catton CN, Jaffray DA, Lebesque JV, van Herk M. *Residual seminal vesicle displacement in marker-based image-guided radiotherapy for prostate cancer and the impact on margin design. Int J Radiation Oncol Biol Phys* 2010 (in press)

Sonke JJ, Belderbos J. *Adaptive Radiotherapy for Lung Cancer. Semin Radiat Oncol* 2010;20:94-106

Steggerda MJ, van der Poel HG, Moonen LM. *Minimizing the number of implantation needles for prostate (125I) brachytherapy: an investigation of possibilities and implications. Brachytherapy* 2010 (in press)

Stewart FA, Hoving S, Russel NS. *Vascular damage as an underlying mechanism of cardiac and cerebral toxicity in irradiated cancer patients. Radiat Res* 2010;174:865-9

Straver ME, Meijnen P, van Tienhoven G, van de Velde CJ, Mansel RE, Bogaerts J, Demonty G, Duez N, Cataliotti L, Klinkenbijn J, Westenberg HA, van der Mijle H, Hurkmans C, Rutgers EJ. *Role of axillary clearance after a tumor-positive sentinel node in the administration of adjuvant therapy in early breast cancer. J Clin Oncol* 2010;28:731-7

## Publications (continued)

Straver ME, Loo CE, Rutgers EJ, Oldenburg HS, Wesseling J, Vrancken Peeters MJ, Gilhuijs KG. *MRI-Model to Guide the Surgical Treatment in Breast Cancer Patients After Neoadjuvant Chemotherapy. Ann Surg* 2010;251:701-7

Straver ME, Meijnen P, van Tienhoven G, van de Velde CJ, Mansel RE, Bogaerts J, Duez N, Cataliotti L, Klinkenbijl JH, Westenberg HA, van der Mijle H, Snoi M, Hurkmans C, Rutgers EJ. *Sentinel node identification rate and nodal involvement in the EORTC 10981-22023 AMAROS trial. Ann Surg* 2010;17:1854-61

Straver ME, Rutgers EJ, Rodenhuis S, Linn SC, Loo CE, Wesseling J, Russell NS, Oldenburg HS, Antonini N, Vrancken Peeters MT. *The relevance of breast cancer subtypes in the outcome of neoadjuvant chemotherapy. Ann Surg Oncol* 2010;17:2411-8

Swellingrebel HA, Marijnen CA, Verwaal VJ, Vincent A, Heuff G, Gerhards MF, van Geloven AA, van Tets WF, Verheij M, Cats A. *Toxicity and complications of preoperative chemoradiotherapy for locally advanced rectal cancer. Br J Surg* 2010;98:418-26

Teertstra HJ, Loo CE, van den Bosch MA, van Tinteren H, Rutgers EJ, Muller SH, Gilhuijs KG. *Breast tomosynthesis in clinical practice: initial results. Eur Radiol* 2010;20:16-24

Topolnjak R, Sonke JJ, Nijkamp J, Rasch C, Minkema D, Remeijer P, van Vliet-Vroegindewij. *Breast patient setup error assessment: comparison of electronic portal image devices and cone-beam computed tomography matching results. Int J Radiat Oncol Biol Phys* 2010;78:1235-43

van Beek S, van Kranen S, Mencarelli A, Remeijer P, Rasch C, van Herk M, Sonke JJ. *First clinical experience with a multiple region of interest registration and correction method in radiotherapy of head-and-neck cancer patients. Radiother Oncol* 2010;94:213-7

van Blitterswijk WJ, Klarenbeek JB, van der Luit AH, Alderliesten MC, van Lummel M, Verheij M. *Fas/CD95 down-regulation in lymphoma cells through acquired alkyllysophospholipid resistance: partial role of associated sphingomyelin deficiency. Biochem J* 2010;425:225-234

(CT<sub>3</sub>) of RT were acquired. The mean seroma volume for CT<sub>1</sub> was 63cc (range: 18-218cc). All patients were planned using the clinical SIB technique (28 x 1.81Gy to the whole breast and additionally 28 x 0.49Gy to the boost volume planned on CT<sub>1</sub>) (SIB) and a SIB<sub>ART</sub> planning technique (like SIB but the first 15 fractions planned on CT<sub>1</sub> and the final 13 on CT<sub>3</sub>). Total dose distributions were projected and evaluated on CT<sub>3</sub>. Seroma reduction was measured between CT<sub>1</sub> and CT<sub>3</sub>. A reduction in the undesired volume receiving  $\geq 95\%$  of the prescribed dose ( $V_{\text{excess}} \geq 50\text{cc}$ ) between the SIB and the SIB<sub>ART</sub>-plan is clinically relevant and feasible considering the expected seroma reduction during RT. Thereby it was set as target for a replan. Of the 21 patients in this study, 10 patients had a  $V_{\text{excess}}$  reduction  $\geq 50\text{cc}$ . These patients all showed an initial seroma  $\geq 40\text{cc}$  and a seroma reduction  $\geq 20\text{cc}$ . If all patients with an initial seroma  $\geq 40\text{cc}$  are monitored, 19% will be monitored unnecessarily. If all monitored patients with a seroma reduction  $\geq 20\text{cc}$  are replanned, 86% will have  $V_{\text{excess}}$  reduction  $\geq 50\text{cc}$ . All patients with  $V_{\text{excess}}$  reduction  $\geq 50\text{cc}$  were monitored and replanned. In this study, the guidelines of monitoring patients with an initial seroma  $\geq 40\text{cc}$  and a replan when they show a seroma reduction  $\geq 20\text{cc}$  is safe. However, whether these thresholds are effective should be addressed in a larger patient group in a future study.

#### Leaf interdigitation and smaller leafs have no significant effect on the quality of VMAT treatment plans

We investigated the effect of interdigitation and leaf width of Elekta MLCs on volumetric modulated arc therapy (VMAT) treatment planning in Pinnacle<sup>3</sup> (Phillips Medical Systems). Three types of MLCs were modelled: 1) An MLC with 1 cm leaves without interdigitation (regular MLC), 2) an MLC with 1 cm interdigitating leaves (interdigit MLC) and 3) a 0.5 cm leaf width MLC with interdigitating leaves (thin MLC). All MLCs have a field of view of 40 by 40 cm<sup>2</sup>. The effect of interdigitation and leaf width is expected to be more pronounced for irregular tumour shapes. Different tumours shapes were studied; prostate and early-stage lung cancer as an example of more spherical PTVs, rectum and head-and-neck tumours for more concave and irregular PTVs. Five patients were randomly selected per tumour site. Treatment plans were generated with the SmartArc module in Pinnacle. Healthy tissue integral dose (ID), dose conformity (CI) and dose homogeneity (DH) in the PTV were compared, where DH is defined as  $(D_{\text{max}} - D_{\text{min}})/D_{\text{mean}}$ . For the various tumour sites, the mean and maximum doses in OARs were evaluated.

The three MLCs have statistically significant different performance, although the differences are small. The performance of the interdigit and thin MLC relative to the regular MLC is summarized in the table; an asterix denotes degradation in performance with respect to the regular MLC. The ID increases for both types of MLC whereas the CI improves. The DH becomes worse for the interdigit MLC and improves for the thin MLC. Stratifying per tumour site points out that these differences were most prominent for rectum and prostate tumours. No statistically significant differences in mean and maximum doses in OARs are observed.

	Relative difference to regular MLC	
	Interdigit MLC	Thin MLC
Healthy tissue Integral Dose (ID)	+ 1.08 %*	+ 0.14 %*
Conformity Index V95% (CI)	- 0.36 %	- 2.34 %
PTV Dose Homogeneity (DH)	+ 2.02 %*	- 10.81 %

Although statistically significant differences in ID, CI and DH were observed, the clinical relevance of the increase in ID and decrease in CI is debatable. No tumour shape dependent improvements were observed. In the case of ID and DH, the interdigit MLC yields poorer results than the regular MLC, in contrast to expectations. It is not yet clear whether this is intrinsically due to the interdigit MLC or to the design of the SmartArc optimization module in Pinnacle.

**Clinical introduction of probabilistic plan evaluation in Pinnacle** An application called UncertLite, which allows for the probabilistic evaluation of a dose distribution, was developed and implemented in Pinnacle. UncertLite simulates the physical

## Publications (continued)

van de Kamer JB, de Leeuw AA, Moerland MA, Jürgenliemk-Schulz IM. *Determining DVH parameters for combined external beam and brachytherapy treatment: 3D biological dose adding for patients with cervical cancer. Radiother Oncol* 2010;94:248-53

van der Molen L, van Rossum MA, Burkhead LM, Smeele LE, Rasch CR, Hilgers FJ. *A randomized preventive rehabilitation trial in advanced head and neck cancer patients treated with chemoradiotherapy: feasibility, compliance and short-term effects. Dysphagia* 2010 (in press)

van Kranen S, van Beek S, Mencarelli A, Rasch C, van Herk M, Sonke JJ. *Correction strategies to manage deformations in head-and-neck radiotherapy. Radiother Oncol* 2010;94:199-205

van Leeuwen FW, Buckle T, Batteau L, Pool B, Sinaasappel M, Jonkers J, Gilhuijs KG. *Potential value of color-coded dynamic breast-specific gamma-imaging; comparing (99m)Tc-(V)-DMSA, (99m)Tc-MIBI, and (99m)Tc-HDP in a Mouse mammary tumor model. Appl Radiat Isot* 2010;68:2117-24

van Lummel M, van Blitterswijk WJ, Vink SR, Veldman RJ, van der Valk MA, Schipper D, Dicheva BM, Eggermont AMM, ten Hagen TLM, Verheij M, Koning GA. *Enriching lipid nanovesicles with short-chain glucosylceramide improves doxorubicin delivery and efficacy in solid tumors. The FASEB Journal* 2010;25:280-9

van Mourik AM, Elkhuizen PHM, Minkema D, Duppen JC, van Vliet-Vroegindewij. *Multiinstitutional study on target volume delineation variation in breast radiotherapy in the presence of guidelines. Radiother Oncol* 2010;94:286-91

van Nes JGH, Putter H, van Hezewijk M, Hille ETM, Bartelink H, Collette L, van de Velde CJH. *Tailored follow-up for early breast cancer patients: a prognostic index that predicts locoregional recurrence. Eur J of Surg Oncol* 2010;36:617-24

Vanneste BG, Haas RL, Bard MP, Rijna H, Váldes Olmos RA, Belderbos JS. *Involved field radiotherapy for locally advanced non-small cell lung cancer: isolated mediastinal nodal relapse. Lung Cancer* 2010;70:218-20

and NTD (with user defined / ) dose distribution for a large number of potential treatments taking into account random and systematic errors, whose distributions are estimated from the clinical IGRT protocol. For a given dose distribution the probability that a certain fraction of a ROI receives a certain dose is calculated within a minute.

UncertLite was distributed in the clinic among experienced technicians, who were asked to plan patients normally. UncertLite was used to check that CTV coverage was sufficient and, in particular when there was overlap between the PTV and an OAR, it was used as an extra aid to choose the best treatment. The UncertLite report was also given to the treating physician.

For 9 prostate patients we found that when the PTV  $V_{95\%} = 99\%$ , 99% of the CTV received on average 95.4% (sd = 0.18%) of the prescribed dose, at 90% confidence. This confirmed our currently used margins, but when introducing new techniques or protocols, UncertLite will be used to re-evaluate them.

As an example where UncertLite helped choosing the best plan, we considered a prostate patient, where the sigmoid colon overlapped with the PTV, making it impossible to meet both the prescribed PTV covering ( $V_{74.1\text{Gy}} > 99\%$ ) and the colon constraint ( $D_{\text{max}} < 70\text{Gy}$ ). Two plans were considered, with characteristics given in the table below. The conventional analysis would favour plan A (higher  $V_{74.1\text{Gy}}$  while  $D_{\text{max}} < 70\text{Gy}$ ). However, using UncertLite, we evaluated the risk associated with insufficient PTV covering and found that the expected dose in the CTV was almost identical for both plans, while the probability that  $D_{\text{max}} > 70\text{Gy}$  was much higher for plan A. Therefore plan B was the better choice for treatment.

Based on the above we concluded that analysis of the dose distribution with UncertLite gives more insight in the true delivered dose and the risks associated with that dose. This insight can be used to check PTV margins and to help deciding on the best planning strategy when sufficient PTV coverage or meeting OAR constraints is not feasible.

	Conventional analysis		UncertLite analysis	
	$V_{74.1\text{Gy}}$ of PTV	$D_{\text{max}}$ sigmoid	Dose in 99% of CTV, with 90% confidence	Probability that max dose in colon $> 70\text{Gy}$
<b>Plan A</b>	90.5 %	69.05 Gy	68.64 Gy	33.6 %
<b>Plan B</b>	86.8 %	68.25 Gy	68.48 Gy	19.5 %

## CLINICAL APPLICATION OF IMAGE GUIDED RADIOTHERAPY

Anja Betgen, Harry Bartelink, Suzanne van Beek, José Belderbos, Nabila Bouzeya, Paula Elkhuizen, Angelo Mencarelli, Jasper Nijkamp, Coen Rasch, Peter Remeijer, Simon Rit, Maddalena Rossi, Christoph Schneider, Rajko Topolnjak, Marcel van Herk, Simon van Kranen, Sandra Vreeswijk, Corine van Vliet-Vroegindewij, Jan-Jakob Sonke

### HEAD AND NECK

#### Plan adaptation for systematic deformations based on average patient model

A new CT is commonly acquired to adapt to progressive anatomy changes during radiotherapy for H&N cancer patients. However, both the planning and the repeat CT are snapshots of a variable patient pose and thus introduce systematic deformations. The purpose of this study was to validate the application of an average patient model.

The average patient model was obtained by the modification of the planning CT with an average deformation vector field (<DVF>) obtained by deformable cone beam CT to planning CT registration over multiple fractions. The following adaptive protocols were compared: online couch shifts (as reference), single plan adaptation with one <DVF> after N scans, and weekly adaptation based on an <DVF> from the previous week. As figure of merit for residual systematic deformations in each protocol, we calculated the average vector length (over all patients) of the average displacement vector (over all fractions) of the bony (B) and soft tissue (ST) landmarks. The effectiveness of single plan adaptation depended on the number of measurements, with an optimum at 12, though the overall effectiveness was modest (B: 2.3→1.5

## Publications (continued)

Verbrugge I, Maas C, Heijkoop M, Verheij M, Borst J. *Radiation and anticancer drugs can facilitate mitochondrial bypass by CD95/Fas via c-FLIP downregulation. Cell Death Differ* 2010;17:551-61

Verheij M, Vens C, van Triest B. *Novel therapeutics in combination with radiotherapy to improve cancer treatment: Rationale, mechanisms of action and clinical perspective. Drug Resist Update* 2010;13:29-43

Witte MG, Heemsbergen WD, Bohoslavsky R, Pos FJ, Al-Mamgani A, Lebesque JV, van Herk M. *Relating Dose Outside the Prostate with Freedom from Failure in the Dutch Trial 68 Gy vs. 78 Gy. Int J Radiat Oncol Biol Phys* 2010;77:131-8

Yang TI, Aukema TS, Van Tinteren H, Burgers S, Valdes Olmos R, Verheij M. *Predicting early chemotherapy response with technetium-99m methoxyisobutylisonitrile SPECT/CT in advanced non-small cell lung cancer. Mol Imaging Biol* 2010;12:174-80

Yang TI, Elkhuzen PH, Minkema D, Heemsbergen W, van Mourik AM, Cassee J, et al. *Clinical factors associated with seroma volume reduction in breast-conserving therapy for early-stage breast cancer: A multi-institutional analysis. Int J Radiat Oncol Biol Phys* 2010;76:1325-32

Yang TI, Minkema D, Elkhuzen PHM, Heemsbergen W, van Mourik AM, van Vliet-Vroegindewij C. *Clinical applicability of cone-beam computed tomography in monitoring seroma volume change during breast irradiation. Int J Radiat Oncol Biol Phys* 2010;78:119-26

mm, ST: 3.6→2.9 mm), indicating progressive changes. Weekly plan adaptation showed an accuracy similar to the validation series (B: 1.2 mm, ST: 2.1 mm) and is expected to perform better on progressive changes. For patients with overall systematic deformations  $\geq 3$ mm, weekly adaptation reduced systematic deformations by more than 45%. Therefore, benefits of the average patient model are expected to be especially for patients with large deformations.

**BREAST**

**Assessment of intra-fraction motion during partial breast irradiation** Recently, a pre-operative image guided accelerated partial breast irradiation (PAPBI) study has started. The purpose of this study was to quantify intra-fraction variability of the target area.

Prior to irradiation, a CBCT is acquired, registered to the planning CT based on grey-values and a correction applied to align the target volume with its planned position for eight patients. A 2nd CBCT is acquired post treatment to determine intrafraction movement. When intrafraction motion exceeding 0.5 cm was observed in any direction, an extra CBCT was acquired halfway within the fraction and was also scheduled for subsequent fractions.

Intrafraction motion was largest in the anterior-posterior direction with  $M=-4$ mm,  $S=3$ mm and  $s=3$ mm. For the other 2 directions intrafraction motion was smaller than 2mm. Due to substantial intra-fraction motion, mid-treatment scans were introduced to limit the impact of intrafraction motion for 50% of the patients.

**LUNG****Four dimensional Cone Beam CT acquisition concurrent with VMAT delivery**

Volumetric modulated arc therapy (VMAT) recently replaced IMRT in stereotactic body radiotherapy (SBRT) for pulmonary lesions in our clinic, considerably reducing treatment delivery times. With both CBCT and VMAT being rotational modalities, concurrent image acquisition and dose delivery became feasible and allows efficient data collection for off-line decision protocols, validation of the patient geometry during actual therapy and detection of intra-fraction motion. The purpose of this work was to evaluate our first clinical experience with simultaneous 4D-CBCT acquisition during VMAT delivery.

Three lung cancer patients with peripheral lesions treated with stereotactic body radiotherapy (SBRT) to 54 Gy in three fractions were included in this study. VMAT plans using two coplanar arcs were optimized using the SmartArc module in Pinnacle3 (Philips, Best, The Netherlands). Plans were delivered on a Synergy treatment machine (Elekta, Crawley, UK) in about 2.5 minutes per arc. For each arc, CBCT projection images (120kV, 20ma, 10 ms) were acquired and reconstructed simultaneously with dose delivery. The reconstruction algorithm keeps up with the image acquisition and produces a 4D scan directly after the delivery of each VMAT arc. These 4D-CBCT scans were displayed over the Mid-Ventilation planning CT scan and visually inspected for tumor misalignments. Post-treatment scans to quantify patient stability that are part of our standard clinical protocol were omitted. Scatter generated from the MV VMAT delivery contributed about 1-2 times as much signal as the kV fluence, and induced vertical streak pattern in the projection images due to the pulsed nature of the treatment beam. Nevertheless, the 4D-CBCT images had adequate image quality and allowed accurate 4D registration of the tumor. Without correction for the extra scatter, the contrast of the bony anatomy relative to soft-tissue, however, was reduced significantly, which affects the automatic bony anatomy registration algorithm. Grey value registration of the bony regions did, however, succeed. So far, concurrently acquired 4D CBCT scans did not lead to interventions. Observed intra-fraction variability of the time averaged tumor position was smaller than 2mm. In conclusion, 4D-CBCT acquisition concurrent with VMAT delivery was successfully implemented for intra-fraction monitoring of SBRT and provides definitive evidence of the treatment quality.

**BLADDER**

**Clinical experience of Image Guided Radiotherapy for bladder cancer based on lipiodol markers** Tumor delineation and localization during treatment is challenging in radiotherapy for bladder cancer. We therefore routinely inject lipiodol markers

around the visible tumor during cystoscopy, as surrogate for the tumor position. The purpose of this study is to evaluate our first clinical experience with online adaptation of radiotherapy based on these lipiodol markers. 14 consecutive patients were evaluated. Lipiodol deposits were clearly visible on both planning CT and Cone Beam CT (CBCT). For all patients, one planning CT and about 25 CBCT scans were acquired. The CBCT scans were first registered to the planning CT on bony anatomy. Then, the lipiodol spots were registered. Both registrations were performed automatically but the lipiodol registration was redone manually if considered unsatisfactory. Translations of the bladder tumor after bone registration were analyzed. Tumor translations after bone registration were 0.07 (0.14), -0.27 (0.63) and -0.01 (0.45) cm in respectively LR, CC and AP direction. The maximum observed translations were 0.90, 1.95 and 2.02 cm, along the 3 axes. We conclude that online adaptation of RT for bladder cancer by lipiodol registration is a feasible and efficient method to reduce the geometrical uncertainties caused by changes in bladder filling variations.

#### 4DCT - high quality imaging and contrast enhancement for 3D radiotherapy treatment planning

4D CT is widely applied to image moving tumors in the lung or the abdomen. For treatment planning the phase closest to the time weighted mean position of the tumor (MidV CT) is an adequate geometric and dosimetric approximation. This procedure, however, is incapable to overcome irregular breathing artefacts, has lower signal to noise (SNR) compared to standard 3DCT and suboptimal contrast enhancement timing. With deformable registration, all 4DCT data can be deformed and used to generate a time-weighted average 3DCT scan, improving the SNR and allowing to overcome breathing artifacts (MidP CT). The purpose of this study was to evaluate usage of a contrast enhanced expiration breath hold (BH) CT as reference in the deformable registration procedure to deform the BHCT to the time weighted average anatomy of the 4DCT.

Deformable registration, based on iterative multi-scale phase-based optical flow was applied to 4D-CT scans of 10 patients, with a BH-scan as reference. The MidP CT was calculated by deformation of each phase to the time weighted average anatomy and subsequently taking the median grey-value over the phases. The MidP BHCT was generated by directly deforming the BHCT to the time weighted average anatomy. Anatomy representation was evaluated by comparing tumor segmentations for each scan. Image quality was evaluated by comparing the SNR in a large vessel at the level of the tumor between the scans.

The MidP CT and MidP BHCT visually contained less imaging artifacts compared to the MidV CT. The average overlap between the segmented tumors in the 3 scans was 88% (range 72-96%) with an average volume of 4.4 cc (range 0.5 - 22.2 cc). In general distances between the segmented edges were in the order of the pixel size, with maxima around 2-3 mm in small sub regions. The average signal in the MidV CT, MidP CT, MidP BHCT no contrast and the MidP BHCT with contrast was 1079, 1078, 1085 and 1197 HU, respectively. The noise found in these scans was 22.8, 8.6, 11.6 and 13 HU, respectively (figure 7).

In conclusion, deforming all image sets derived from clinical 4D-CT-scans to a MidP-CT is a robust technique and is about to be introduced in our clinic. Subsequently, addition of expiration breath hold contrast enhanced imaging to create a MidP BHCT facilitates optimal contrast timing in 4D workflows. The MidP BHCT can facilitate for more accurate and reproducible delineation of involved lymph nodes.

Figure 7: Overview of the image quality in the mediastinal region when using a MidV-CT (left), a MidP-CTRef\_5 (middle) and a MidP-BH-CT (Right) at exactly the same level and window settings



## PROSTATE

### Hybrid registration technique for image-guided radiotherapy of prostate cancer

Fiducial markers are an accurate surrogate for the prostate, but they provide little information on the position of the seminal vesicles (SVs). To reduce the SV position uncertainty we propose a hybrid registration technique that uses fiducial markers to localize the prostate and subsequently performs a gray-value registration to correct for the orientation of the SVs. Fifteen prostate cancer patients were implanted with two or three 0.35 x 20 mm gold markers. Gray-value registration of the delineated SVs was started from the marker registration, allowing only rotations around the left-right (LR) axis. The center of mass of the prostate was chosen as center of rotations. We validated the SV registration by calculating residual registration errors for three clearly identifiable landmarks (small calcifications) present in the SVs of three patients. The SVs of eight patients showed a substantial ( $>5^\circ$ ) mean LR rotation relative to the marker registration. Overall, we found  $M = -3.0^\circ$ ,  $\sigma = 6.2^\circ$  and  $\tau = 5.0^\circ$ . These results confirm that substantial differences between prostate and SV orientation exist. Out of 398 scans, the SVs of 41 scans could not be registered automatically, mostly due to motion artifacts in the CBCT image. For most cases, there was a decrease in registration error, especially for large differential SV rotations.

Correction, e.g. using collimator rotations, would improve target coverage of the SVs and spare organs at risk, while preserving the planned dose to the prostate.

## BREAST CANCER

Femke van der Leij, Marc van de Vijver<sup>1</sup>, Jelle Wesseling, Kenneth Gilhuijs, Hester Oldenburg, Claudette Loo, Adrian Begg, Wouter Vogel, Sandra Vreeswijk, Corine van Vliet-Vroegindeweij, Harry Bartelink, Paula Elkhuisen

<sup>1</sup> AMC, Department of Pathology, Amsterdam

## DEFINING RADIOTHERAPY SENSITIVITY

### A. Image guided Preoperative Accelerated partial Breast Irradiation (PAPBI)

Radiotherapy is part of breast conserving therapy (BCT) and is known to reduce LR rates in all patients by 60-70%. So far, no patient groups can be defined in whom radiotherapy would not be necessary. It is estimated that in approximately half of the patients whole breast radiotherapy is not necessary, while in others the tumor might be resistant to radiotherapy. If it would be possible to predict tumor response to radiotherapy, a more tailored treatment can be advised to individual patients (higher boost dose or primary mastectomy). To evaluate the in situ breast radiosensitivity, the image guided accelerated partial breast irradiation (PAPBI) is the best scheme of irradiation because of (i) low breast / ratio suggesting that breast cancer is more sensitive to high dose per fractions; (ii) very precise breast tumor irradiation; (iii) limited volume of irradiated area allowing larger fractions with no extra risk on late toxicities; (iv) short treatment time course.

This trial is directed at implementing pre-operatively given image guided accelerated partial breast irradiation without compromising local control in early breast cancer patients. By assessing tumor response to radiotherapy, the goal of the study is to develop a gene expression profile that predicts the breast cancer radiosensitivity.

This gene signature of breast radiosensitivity would further design optimal treatment strategies for individual breast cancer patients treated with BCT

To qualify for the trial, patients must be 60 years or older, and have an unifocal cT1-2 ( $\leq 3$ cm) pN0 Mo breast cancer; sentinel node procedure before irradiation. Patients will be treated by a preoperative APBI (PAPBI) consisting in delivering 10 x 4 Gy over 12 days. Six weeks after PAPBI, a wide local excision will be performed. As the tumor remains 'in situ' during irradiation, accurate tumor delineation and control of accurate radiation dose delivery to the tumor becomes possible by treating these patients with a cone beam CT linear accelerator. To identify a subgroup of breast cancer radiosensitivity, biological studies planned are gene expression profiling from RNA and DNA isolated from biopsies and fine needle aspiration taken of the tumor before, during radiotherapy and at time of operation. The mRNA gene expression profiles, the miRNA expression profiles and the DNA copy number changes will be

correlated with response to radiotherapy, defined as pathologic response at the time of the lumpectomy (i.e. 6 weeks after the completion of the PAPBI). Response of the tumor will be evaluated by MRI scan and PET (before radiotherapy and before surgery) and classical pathology.

The trial, which started accrual yet, will accrue 120 patients in total over a period of years. First, 60 patients will be studied as a test set to identify predictive profiles and then, 60 patients more will be used as a validation set.

Other important aspects of this study are collections of fresh frozen tumor tissue, blood and urine samples (i) to assess the radio-induced genetic alterations on the surgical post-radiation specimen compared to the tumor response 6 weeks after the end of radiotherapy; (ii) to study the early changes in gene-profiling and (iii) to evaluate the early functional imaging modifications. The Institut Gustave Roussy (France) and the Karolinska Institutet (Sweden) will participate in this study (Descartes Cancer Consortium).

#### B. Radiosensitivity breast cancer cell lines

In addition with the clinical PAPBI study, 30 human breast cancer cell lines will be investigated for their radiosensitivity profile. This will also be implemented in the study described in D.

#### C. Case control study focusing local recurrence

Genetic profiling will be studied in 240 breast cancer patients (79 cases with 161 matched controls). This study is in association with Institut Curie from France. The results will also be implemented in the study described in D.

D. In the running Young Boost Trial over 1200 patients under 50 years have been randomized between normal boost dose vs. a higher boost dose after breast-conserving therapy. From these patients frozen material as well as paraffin embedded material is collected. Follow up is available for the first years. The profiles found in the studies A-B to be related with radioresponse will be evaluated on this material whether a response profile eventually is associated with local control. In addition, the results from the case-control study will be evaluated on this cohort.

## COMBINATION OF RADIOTHERAPY AND CHEMOTHERAPY/BIOLOGICALS

Berthe Aleman, Harry Bartelink, Jos Beijnen, José Belderbos, Henk Boot, Annemieke Cats, Frits van Coevorden, Ewout Courrech Staal, Otilia Dalesio, Maarten Deenen, Luc Dewit, Johan Dikken, Ria Dubbelman, Wilma Heemsbergen, Michel van den Heuvel, Frans Hilgers, Edwin Jansen, Rianne de Jong, Joost Kneijens, Maria Kuiper, Corrie Marijnen, Lisette van de Molen, Coen Rasch, Maurits Swellengrebel, Renato Valdes Olmos, Johanna van Sandick, Jan Schellens, Karijn Verschueren, Vic Verwaal, Marcel Verheij

**Head and neck** The CONDOR cooperative trial the University of Nijmegen targets patients below 60 years with stage III/IV head and neck cancer and is open since 2008. Patients are first to receive 3-4 courses of TPF chemotherapy followed by a randomization between two regimens of chemoradiation. Nineteen of 70 patients have entered the trial so far.

The final report on the quality of life for patients with chemoradiation treated within the M99RAD trial is submitted. Results remain favorable compared to historical series with smaller tumor treated with surgery and radiotherapy. Quality of life before treatment and after one year is predictive for (disease specific-) survival. Based on our preclinical research on apoptosis-modulation, we have initiated a clinical phase I-II trial in locally advanced head and neck cancer combining standard cisplatin-based chemoradiotherapy with dose escalating AT-101, a small molecule inhibitor of anti-apoptotic Bcl-2/Bcl-XL. To date, 7 patients have been included.

**Gastroenterology – Esophageal cancer** Over recent years a database was set up including data on all patients treated for esophageal cancer in our institute since 1997 (approximately 1500 patients). We evaluated the toxicity and efficacy of three different regimens of concurrent chemoradiation (CRT) in 94 patients with esophageal cancer treated between 1997 and 2007. Treatment consisted of radiotherapy to 50 Gy in 25 fractions with concurrent cisplatin and 5-fluorouracil (group A, n=65), radiotherapy to 50.4 Gy in 28 fractions with concurrent carboplatin

and paclitaxel (group B, n=16) or radiotherapy to 66 Gy in 33 fractions with low-dose cisplatin (group C, n=13). Toxicity was scored according to CTC v.3.0. Chemoradiation was planned as neoadjuvant (n=58) or definitive (n=36) treatment. Grade 3/4 hematological toxicity occurred in 18 (19%) patients and grade 3 non-hematologic toxicity in 8 (9%) patients. During treatment, 2 patients died (1 from duodenal ulcer bleeding and 1 from stroke). Overall, 81 (86%) patients completed the planned treatment (86%, 94%, and 77% in groups A, B, and C, respectively). Clinically complete or partial response was observed in 28 of 92 (30%) patients (21%, 50%, and 54% in groups A, B, and C, respectively). After clinical and radiologic response evaluation, treatment plan was changed in 14 (15%) patients. A total of 45 patients underwent surgery. Pathologic complete response and downstaging were seen in 12 (27%) and 34 (76%) operated patients, respectively. With a median follow-up of 15 (range, 1-108) months, the 3-year survival was 41% for all patients. We conclude that with individual treatment planning, different regimens of chemoradiation for esophageal cancer resulted in acceptable rates of toxicity and efficacy.

**Gastroenterology – Gastric cancer** In the US Intergroup 0116 study, a significant survival benefit in postoperative CRT was reported in gastric cancer. Based on these results we completed three adjuvant chemoradiotherapy phase I-II trials in gastric cancer. From these trials we identified the regimen for the experimental arm in the CRITICS study. In this international randomized phase III study patients with operable gastric cancer receive preoperative chemotherapy, surgery and postoperative chemotherapy, or preoperative chemotherapy, surgery and postoperative CRT. At this moment over 300 patients have been randomized. In addition to Sweden that joined the trial in 2008, Denmark participates as well since ultimo 2010. Furthermore, we are running a phase I-II study together with the AMC and VUmc, in which neoadjuvant chemoradiation with weekly paclitaxel and capecitabine is applied in patients with inoperable gastric cancer. So far, 10 patients have been included in this NARCIS trial.

In collaboration with Prof Van de Velde from the LUMC, we analyzed the impact of the extent of surgery and postoperative chemoradiotherapy on recurrence patterns in gastric cancer. We retrospectively compared survival and recurrence patterns in our phase I/II studies evaluating more intensified postoperative CRT with those from the Dutch Gastric Cancer Group Trial (DGCT) that randomly assigned patients between D1 and D2 lymphadenectomy. Survival and recurrence patterns of 94 patients with adenocarcinoma of the stomach who had received surgery followed by radiotherapy combined with fluorouracil and leucovorin (n=5), capecitabine (n=39), or capecitabine and cisplatin (n=50) were analyzed and compared with survival and recurrence patterns of 694 patients from the DGCT (D1, n=369; D2, n=325). With a median follow-up of 27 months in the CRT group, local recurrence rate after 2 years was significantly higher in the surgery only (DGCT) group (17% v 5%; p=0.0015), while no significant differences were found for overall survival at 2 years (67% v 70%). Separate analysis of CRT patients who underwent a D1 dissection (n=41) versus DGCT-D1 (n=369) showed fewer local recurrences after chemoradiotherapy (2% v 18%; p<0.01), whereas comparison of CRT-D2 (n=25) versus DGCT-D2 (n=325) demonstrated no significant difference. CRT significantly improved survival over surgery only after D1 dissection (83% v 73%; p=0.04), but not after a D2 dissection (59% v 63%). In the subgroup of patients who underwent a microscopically irradical (R1) resection, CRT significantly reduced local recurrences and improved survival (3% v 21%; p=0.02 and 68% v 30%; p<0.01, resp.). Thus, after D1 surgery or R1 resection, the addition of postoperative CRT had a major beneficial impact on local recurrence and survival in resectable gastric cancer.

In collaboration with the departments of Clinical Pharmacology and Pharmacy & Pharmacology (Slotervaart Hospital) we determined the effect of gastric surgery and radiotherapy (RT) on the exposure to capecitabine and its main metabolites DFCR and DFUR in gastric cancer patients. 84 pts with non-metastasized, adenocarcinoma of the stomach or gastro-esophageal junction received a partial (n=45)/total (n=26) gastrectomy or esophagocardiac (n=13) resection followed by standard

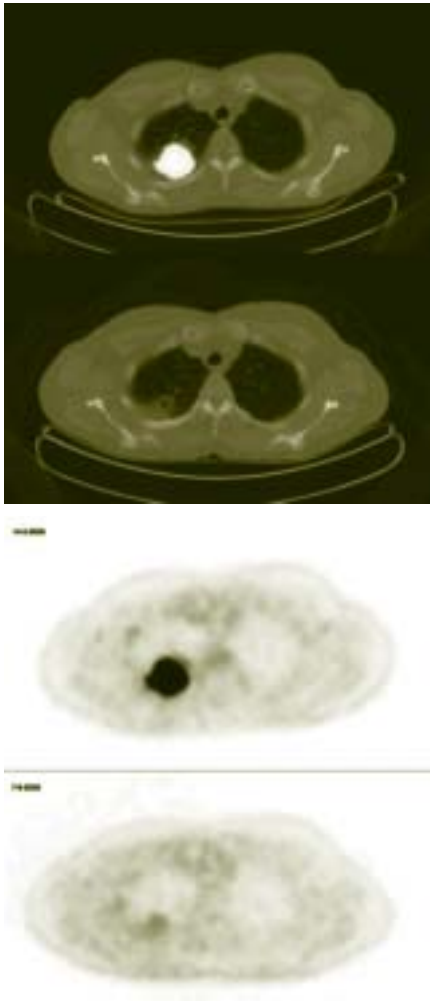
postoperative adjuvant capecitabine-based CRT. Blood samples were drawn on days 22 and 43 to determine the pharmacokinetics (PK) of capecitabine, DFCR and DFUR, and were analyzed using LC-MS/MS. 18 anal cancer patients with an intact stomach treated with similar doses of capecitabine served as a control group. PK of capecitabine, DFCR and DFUR showed wide inter- and low intra-patient variability. There was no significant effect of daily radiation on the exposure to capecitabine and metabolites. Total and partial gastrectomy resulted in increased AUC and Cmax of capecitabine and metabolites, whereas Tmax was earlier. Clinical consequences of this variability have to be assessed.

**Gastroenterology – Rectal cancer** Pre-operative capecitabine-based chemoradiotherapy (CRT) has become standard treatment in locally advanced rectal cancer. We evaluated acute toxicity and surgical complications in these patients following total mesorectal excision (TME) after preoperative CRT with capecitabine. Between 2004 and 2008, 147 consecutive patients with clinical tumour category (cT) 3-4 (with a threatened circumferential resection margin or cT3 within 5 cm of the anal verge) or clinical node category 2 rectal cancer were treated with preoperative CRT (50 Gy, capecitabine 825 mg/m<sup>2</sup> twice daily, days 1-33). TME followed 6 weeks later. Toxicity was scored according to the CTC (version 3.0) and RTOG scoring systems. Treatment-related surgical complications were evaluated for up to 30 days after discharge from hospital using the modified Clavien-Dindo classification. The mean cumulative dose of capecitabine was 95% and 98% of patients received at least 45 Gy. One patient died from sepsis following haematological toxicity. Grade 3-5 toxicity developed in 32 patients (22%), in particular diarrhoea (10%) and radiation dermatitis (12%). There were no deaths within 30 days after surgery. Anastomotic leakage and perineal wound complications developed after 13 of 47 low anterior resections and 23 of 62 abdominoperineal resections. Surgical reintervention was required in 30 patients. Twenty-seven patients (20%) of 138 patients who had a laparotomy were readmitted within 30 days after initial hospital discharge. We concluded that preoperative CRT with capecitabine is associated with acceptable acute toxicity, significant surgical morbidity but minimal postoperative mortality.

**Gastroenterology – Anal cancer** The feasibility and efficacy of simultaneous integrated boost – intensity modulated radiation therapy (SIB-IMRT) with concomitant capecitabine and mitomycin-C was investigated in a phase I dose-finding study in 18 patients with locally advanced anal cancer. Patients with locally advanced anal carcinoma were treated with SIB-IMRT in 33 daily fractions of 1.8 Gy to the primary tumor and macroscopically involved lymph nodes and in 33 fractions of 1.5 Gy electively to the bilateral iliac and inguinal lymph node areas. Mitomycin-C 10 mg/m<sup>2</sup> was administered on day 1, and capecitabine was given in a dose-escalated fashion twice daily on irradiation days, until dose-limiting toxicity emerged in ≥ 2 of 6 patients. An additional eight patients were treated at that dose level. Patients received a sequential radiation boost dose of 3 x 1.8 Gy if macroscopic residual tumor was still present in week 5 of the radiation treatment. In total, 18 patients completed the planned treatment. The MTD was capecitabine 825 mg/m<sup>2</sup> BID. The most predominant acute toxicities (all grades) included dermatitis within the radiation area (100%), fatigue (83%), pain (72%), diarrhea (67%), and leukocytopenia (61%). Grade ≥ 3 toxicities were dermatitis (72%), fatigue (22%), and hyponatremia (11%). Of all patients, 72% (95%-CI: 51-94%) achieved a complete response, and 28% had a partial response. In none of the complete responders, a relapse was observed after a median follow-up of 18 months. Longer follow-up is needed to assess the long-term effects of this treatment.

**Lung - NSCLC** Combining concurrent chemotherapy with radiotherapy (CRT) is the standard treatment of locally advanced NSCLC. Currently we are accruing patients in the RADITUX trial (M07CCL). In this multi-center randomized phase II trial patients with inoperable locally advanced NSCLC are randomized to our CRT regimen (66 Gy in 24 fractions and daily dose Cisplatin 6 mg/m<sup>2</sup>) with or without the weekly addition of an EGFR monoclonal antibody (Cetuximab). The addition of Cetuximab to our concurrent CRT was well tolerated in a phase I trial. Between January and November 2010, 25 patients were treated within this trial in the NKI-

Figure 8: Partial Metabolic response in an 53 year old female with cT3No NSCLC shortly after chemoradiation with cetuximab (M07CCL)



AVL (total inclusion: 93 patients). We expect to complete this trial in the first half of 2011. In this group of patients, we studied the esophagus toxicity using FDG-PET images to correlate radiotherapy dose to esophageal toxicity (figure 8).

Dose-escalation is studied by boosting radiation dose within the primary tumor applying non-uniform radiation dose distribution using IMRT to the target based upon biological activity on pre-treatment FDG-PET scan. In collaboration with Prof de Ruyscher from the MAASTRO clinic the phase II PET boost trial (M09PBO) opened in 2010. Patients are randomized to dose escalation to the planning target volume of the primary tumor as a whole or to the 50% SUVmax of the primary tumor (of the pre-treatment FDG-PET scan). The patients receive concurrent chemotherapy if feasible. The primary objective is to determine the local progression free survival at 1 year. In both treatment arms, the patients are irradiated to the same maximum tolerated dose to the lung. Until November 2010, 8 patients were randomized (4 patients from the NKI-AVL).

**Lung - SCLC** Approximately 20% of malignant tumors of the lung are due to small cell carcinoma. In general, these patients carry a worse prognosis compared to NSCLC patients. For limited stage small cell lung cancer (LS-SCLC), the combination of chemotherapy and thoracic radiotherapy is the standard treatment. Two meta-analyses have shown that thoracic radiotherapy given concurrently with chemotherapy improves both survival and local control. Nevertheless, several important questions including the optimal total radiation dose and radiation fractionation are still unanswered. To establish a standard chemo-radiotherapy regimen for LS-SCLC, an EORTC international, multicenter randomized phase III trial started in 2009 comparing twice daily radiotherapy with high dose radiation delivered once daily (CONVERT trial). To date, a total of 139 patients were treated within this trial (2 patients from the NKI-AVL). For extensive stage small cell lung cancer (ES-SCLC), chemotherapy is the cornerstone of treatment. However, over 75% of patients have persisting intra-thoracic disease after initial chemotherapy, and about 90% manifest intra-thoracic disease progression at 1 year after completing initial chemotherapy. In the absence of promising systemic agents that can improve local response, the role of thoracic irradiation in patients with ES-SCLC is currently being evaluated in a multicenter phase III randomized trial (CREST trial). The objective of this study is to investigate whether thoracic radiotherapy can improve 1-year survival, following a response to chemotherapy. A total of 120 patients have now been treated within this trial. At the NKI-AVL, patient accrual started in September 2009 and to date 16 patients have been included.

## BRACHYTHERAPY

Berthe Aleman, Marcel Steggerda, Baukelien van Triest, Thelma Witteveen, Simon Horenblas, Floris Pos, Luc Moonen

**Bladder preservation with brachytherapy for bladder cancer** This year we have updated the clinical outcome as part of a joint effort to analyze the results of all bladder cancer patients treated with brachytherapy in the Netherlands. The data have been sent to the central database, which is located at the department of Radiotherapy in the Academic Medical Center in Amsterdam. The results of the joint analysis are expected in 2011.

In recent years, we have updated and implemented several new techniques for bladder cancer brachytherapy. A new initiative in close cooperation with the department of urology is the implementation of minimal invasive surgery. In Arnhem, they have developed a laparoscopic implantation procedure, which is already a major improvement. The "Arnhem" procedure might be even further improved by the implementation of robotic assisted laparoscopic implantation. This technique is currently being developed; the first patients will be treated in the first half of 2011. The impact for the mostly elderly bladder patients will be enormous. It is expected that the hospitalization, which is usually 7 – 10 days, can be reduced to 3 days.

**Focal brachytherapy for prostate cancer** In the last decade, there has been a large increase in the detection rate of prostate cancer and a significant increase in the proportion of men with very early organ confined disease. At present, all established local forms of prostate cancer therapies, such as brachytherapy, aim at treating the entire prostatic gland. Although highly effective, these treatments are associated with significant morbidity (i.e. erectile dysfunction, urinary incontinence/problems etc.) and can seriously affect the quality of life.

Attempts to treat only one side of the prostate (based on biopsy proven unilaterality) or exclusively the dominant cancer focus (detected by MRI scans) gain growing interest. Preliminary results of several small studies using cryotherapy or High-Intensity Focused Ultrasound (HIFU) applied to part of the prostate show an important reduction of morbidity rates.

Focal or partial prostate brachytherapy seems a logical step. As no other form of prostate cancer therapy, it is possible to focus the treatment to a part of the prostate only. Before focal brachytherapy becomes feasible, there is need of high quality imaging. Together with the department of radiology and in close cooperation with Utrecht University hospital, we have implemented state of the art high quality 3 Tesla MRI sequences. We are now able to identify a dominant lesion in > 50 % of the brachytherapy candidates. Furthermore, we have integrated MRI in the brachytherapy process and have done focal brachytherapy treatment planning on these patients to evaluate feasibility of the procedure. Now we are ready to implement focal brachytherapy in the clinic. We are currently working on a phase II study evaluating focal brachytherapy in early stage prostate cancer.

## MECHANISMS, MODULATION AND PREDICTION OF RADIATION-INDUCED CELL DEATH

Maaïke Alderliesten, Wim van Blitterswijk, Jannie Borst, Albert van Hell, Gerben Koning<sup>1</sup>, Dayane Martins, Rogier Rooswinkel, Renato Valdes Olmos, Baukelien van Triest, Conchita Vens, Shuraila Zerp, Marcel Verheij

<sup>1</sup> Erasmus MC, Rotterdam the Netherlands

The translational research performed within our group focuses on (1) the identification and preclinical testing of novel targets and agents to enhance the cytotoxic effect of radiation and on (2) the validation of new endpoints and clinical biomarkers to quantify and predict the efficacy and toxicity of new combination therapies. The ultimate objective is to rapidly translate these strategies from the lab into the clinic.

In close collaboration with several research groups within the NKI, new agents are identified on the basis of their mechanism of action and subsequently tested for their ability to induce apoptotic cell death and to increase the cytotoxic effect of radiation in vitro and in vivo. Current research projects focus on synthetic alkyl-phospholipids (Edelfosine, Perifosine, Erucyl-PC), death receptor ligands (TRAIL, CD95L/FasL/APO010), small molecule inhibitors of Bcl-2 (Gossypol/AT-101, ABT-737) and DNA damage repair inhibitors (Olaparib, APO866). To monitor tumor response and predict treatment outcome, we explore new functional imaging modalities including in vivo imaging of apoptosis by annexin V scintigraphy, MIBI SPECT-CT and ML-10 ApoSense.

In a separate project we investigate the patented concept of improved drug delivery by short chain sphingolipid-enriched liposomes in vitro and in vivo.

**Alkyl-phospholipids (APLs)** APLs represent a first group of compounds that has become available for clinical application along this translational approach. These synthetic anti-tumor agents are known to accumulate in sphingomyelin- (SM) and cholesterol-enriched plasma membrane microdomains, also known as “lipid rafts”. Once taken up via these membrane portals, APLs interfere with lipid metabolism, inhibit proliferative and survival signaling, affect cell cycle distribution and stimulate apoptosis induction in a variety of tumor cell systems. In combination with radiation, APLs cause a synergistic apoptotic effect and reduce clonogenic cell survival.

The synthetic APL Edelfosine (1-O-octadecyl-2-O-methyl-rac-glycero-3-phosphocholine) induces apoptosis in S49 mouse lymphoma cells. Variant cells, S49AR, made resistant to APL, show impaired APL uptake through lipid rafts and are SM deficient. These cells display cross-resistance to other apoptotic stimuli, such as Fas/CD95 ligand (FasL) and DNA damage (etoposide, radiation), but they can be gradually resensitized (S49ARS cells) by prolonged culturing in the absence of APL. The resistant S49AR cells show constitutively enhanced levels of phospho-ERK and phospho-Akt/Protein kinase B, characteristics of survival signaling. Pharmacological inhibition of these enzymes restored apoptosis sensitivity towards DNA damage, but not to APL or FasL. In search for a common mediator of the cross-resistance, upstream of Akt, we found that S49AR lacked SHIP-1, an SH2 domain-containing inositol phosphatase that converts the Akt activator PtdIns(3,4,5)P<sub>3</sub> to PtdIns(3,4)P<sub>2</sub>. Using <sup>32</sup>P-radiolabeling and HPLC, we confirmed that these phosphoinositide levels changed accordingly. Resensitized S49ARS cells regained SHIP-1 expression and showed normalized levels of phosphoinositides and SM, like the parental S49 cells. Down-regulation of SHIP-1 using siRNA resulted in (partial) apoptosis cross-resistance, SM deficiency and shift in phosphoinositide levels, much like we found in S49AR cells. Our present and previous results suggest that SHIP-1, in yet unresolved interplay with SM synthase-1, mediates apoptosis sensitivity of S49 lymphoma cells towards APL, FasL and DNA damage.

Perifosine (PER) is another, orally available, membrane targeting APL and Akt inhibitor with preclinical radiosensitizing, apoptosis-enhancing and anti-angiogenic properties. In a previous phase I study we established the MTD and optimal scheduling of PER in combination with radiation (RT). We recently conducted a randomized, double-blind, placebo-controlled multicenter phase II study to assess the efficacy of daily PER and RT in patients with locally advanced NSCLC. Secondary objectives were to determine the toxicity of this regimen, and to evaluate systemic exposure of the drug during RT. A total of 177 patients from 19 centers were entered. Stages: IA-B (4.6%), IIB (9.6%), IIIA (37.3%), IIIB (48.6%). Of these patients 95 received PER (53.7%) and 82 placebo (46.3%; PLA). 121 patients (65 PER; 56 PLA) entered the study without prior chemotherapy and 56 (30 PER; 26 PLA) had prior chemotherapy. The primary endpoint could not be evaluated as only 15% of the patients reached the 1-year follow up. Response evaluation at day 65 showed an overall RR (CR+PR) of 40% and was not significantly different between both arms (PER: 42% and PLA: 38%). For the subgroup of patients without prior chemotherapy TLF indicated an advantage for the PER group (mean 230 vs 165 days; median 206 vs 126 days). Kaplan-Meier survival curves indicated an advantage for PER patients without prior chemotherapy ( $p=0.088$ ). In both groups, the majority of patients reported treatment related AEs (PER 86.3%; PLA 76.8%). The most frequently observed toxicity in the PER group was gastro-intestinal (grade 3-4: 14.7% vs PLA 4.9%). Plasma concentration of PER on the first and last day of RT were comparable and in the same range as determined previously. We concluded that the high number of patients who did not reach the 1 year follow up, mainly due to systemic progression, compromised the power of the trial to detect an effect of the study treatment on the local control rate. A small advantage for TLF and survival was observed in the PER group without prior chemotherapy. Gastro-intestinal toxicity was the most frequently observed PER-related side effect.

Other promising APL derivatives with potentially better bioavailability and radiosensitizing properties, like the i.v. compound Erucyl-PC, have become available and are studied in vitro and in vivo.

**Other radiosensitizers in preclinical development** In two separate projects with J Borst (Division of Immunology) we study other radiosensitizers. A long term line of research focuses on the interaction between death receptor ligands (TRAIL and MegaFasL/APO010) and DNA damaging regimens (radiation and etoposide). TRAIL induces apoptosis in a wide variety of tumor tissues, but lacks normal tissue toxicity in preclinical animal models. In several leukemic and solid tumor cell lines, we demonstrated combined (additive to synergistic) effects of TRAIL + radiation/etoposide. The effectiveness and acceptable toxicity of the combined treatment of

TRAIL and radiation was subsequently demonstrated *in vivo*. These experiments have been expanded with another death receptor ligand (MegaFasL/APO010). Our current studies focus on the impact of TRAIL death receptor trafficking on pro-apoptotic signaling.

In collaboration with the University of Michigan and the division of Radiobiology at the Free University of Amsterdam, we have initiated preclinical efficacy testing of small-molecule inhibitors of anti-apoptotic members of the Bcl-2 family (AT-101 and ABT-737). Currently, the combination of AT-101 with cisplatin-based chemoradiotherapy is evaluated in a clinical phase I/II study in locally advanced head and neck cancer. So far, 7 patients have been included and no DLT has been observed.

ABT-737 has been chemically designed to specifically interact with anti-apoptotic Bcl-2 family members through binding to their BH3-interacting domains prohibiting interactions with their pro-apoptotic relatives Bax and Bak and with other BH3-only proteins. We are investigating under which conditions ABT-737 might synergize with radiation and etoposide using enforced expression of the 6 different anti-apoptotic proteins in Jurkat and Molt-4 acute lymphoblastic T cells. In cases where cells became resistant to radiation, this could be counteracted by the addition of ABT-737. For the reverse we showed that synergy only occurs upon upregulation of specific Bh3-only proteins. The importance this upregulation was confirmed using cells that express these proteins in an inducible way. Together, these results allow us to make an *a priori* prediction about which treatments to combine with ABT-737 based on the bcl-2 protein status of a tumor.

In collaboration with C Vens (Division of Experimental Therapy) we explore the interaction between radiation and inhibitors of DNA repair. The NAD<sup>+</sup>-depleting agent APO866 was found to enhance radiation-induced cell death and act as a radiosensitizer in various models, including 2 prostate cancer cell lines. Restoration of cellular NAD levels abolished the cytotoxic effect. *In vivo* MTD of APO866 was defined as the highest non-lethal dose with a reduction in body weight of less than 10%, and was determined at 10 mg/kg, administered every 12 hours for 4 times. APO866 induced NAD-depletion is thought to inhibit PARP, that is involved in DNA repair. PARP inhibitors are also good candidates for combined use with DNA damaging agents. The main mechanism by which both radiation and cisplatin kill tumor cells is by an accumulation of un- or misrepaired DNA damage. PARP inhibitors increase radiation and chemotherapy (Cisplatin) response in preclinical studies. PARP inhibitors have been shown to specifically kill homologous recombination deficient tumor cells as single agent. ATM mutations are expected to affect DSB repair and homologous recombination status therefore amplifying damage induced by the combined PARP inhibitor radiation (Cisplatin) treatment. Thus tumor targeted treatment and radio-chemosensitization could be achieved in the presence of frequently observed ATM gene mutations. We have designed 3 phase I-II studies evaluating the safety and tolerability of Olaparib in combination with (cisplatin-based chemo-) radiotherapy in locally advanced breast cancer, NSCLC and head and neck cancer. Olaparib exhibits low systemic toxicity profiles when given as monotherapy. When combined with chemotherapeutic agents more toxicity is seen.

**Prediction of tumor response** Radiation, like most anti-cancer treatments, achieves its therapeutic effect by inducing different types of cell death in tumors. To monitor treatment efficacy a variety of routine anatomical imaging modalities is available. However, changes in tumor function (e.g., metabolism, proliferation, hypoxia) often precede these volumetric alterations and may reflect tumor responses to treatment more accurately. Therefore, reliable biomarkers and imaging modalities that could assess treatment responsiveness in an early phase would be very useful to identify responders and/or avoid ineffective, toxic therapies. We previously evaluated two non-invasive cell death imaging techniques in collaboration with the department of nuclear medicine (Valdés Olmos, Division of Diagnostic Oncology): 99mTc-Annexin V scintigraphy (TAVS) and 99mTc-MIBI single photon emission computed tomography (MIBI SPECT-CT). Our results indicated that both TAVS and MIBI SPECT-CT might be useful as non-invasive predictive tests for treatment outcome,

ultimately allowing an early adaptation of the initiated therapy and help to design novel (combined modality) strategies. Currently, we focus on another potential imaging biomarker for radiation-induced cell death:  $^{18}\text{F}$ -ML-10. We designed a clinical protocol in rectal cancer to determine the optimal timing of ML-10 imaging for predicting treatment outcome after preoperative 5x5 Gy or capecitabine-based chemoradiotherapy (25x2 Gy).

**Improved in vitro and in vivo anti-tumor efficacy of glucosylceramide-enriched liposomal doxorubicin** Anti-cancer therapy is often suboptimal due to inability to deliver sufficient levels of cytostatics into tumor cells. We identified a class of short-chain sphingolipids that, when inserted in the tumor cell membrane, facilitates the translocation of certain drugs of well-defined amphiphilicity over the plasma membrane. One of these sphingolipids, N-octanoyl-glucosylceramide (GC), co-formulated with liposomal doxorubicin, enhanced the accumulation of doxorubicin into cultured tumor cells and into xenograft tumor tissue in vivo. This translated in enhanced anti-tumor efficacy of the GC-enriched doxorubicin liposomes in an A431 xenograft tumor model. Next, we examined this novel concept of GC-directed membrane permeabilization for doxorubicin in a spontaneous mouse tumor model that mimics human Invasive Lobular Carcinoma (ILC) breast cancer. We found that GC-enriched liposomal doxorubicin enhanced the uptake of doxorubicin in ILC cell cultures at least five-fold, and inhibited tumor outgrowth in vivo much more effectively than either of the two clinically applied formulations of doxorubicin, (free, non-liposomal) Adriamycin® or (standard/conventional liposomal) Caelyx®. Mice treated with GC-liposomal doxorubicin showed an extended overall survival (up to 2-fold) compared to conventional liposomes (figure 9). No increase in normal tissue toxicity was observed upon the addition of GC. The presented data hold promise for widening the therapeutic window of amphiphilic anti-cancer agents, including doxorubicin, using this plasma membrane modulation strategy. We are currently continuing the GC-enriched liposomal doxorubicin towards clinical investigation. Moreover, we investigate the cellular and molecular mechanisms of GC-directed membrane permeabilization. The facilitation of doxorubicin influx by short-chain sphingolipids appeared dependent on the (cellular) lipid membrane environment. Insertion of the short-chain sphingolipids into plasma membranes does not result in enhanced doxorubicin accumulation in any cell type. Cardiac myocytes, for example, do not respond to GC exposure, in contrast to all malignant cells that have been tested. In order to pinpoint the specific membrane requirements that are involved, we have set-up a membrane model system that allows studying the translocation of doxorubicin over lipid membranes of various compositions. In addition, we are examining the specificity of the GC for particular cell types, focusing on the in vivo accumulation of doxorubicin in heart and (spontaneous) tumor tissue, cardiac function upon repeated administration, and the overall toxicity profile of this new GC-enriched doxorubicin formulation.

Figure 9: GC co-formulation improves the overall survival in mice with progressing ILC. Mice received no treatment (control, purple line), once weekly free doxorubicin (bleu line), conventional liposomal doxorubicin (yellow line) or the GC-modified liposomal doxorubicin (green line). A body weight decrease to 80% of the initial value at start of treatment or a tumor volume exceeding 1500 mm<sup>3</sup> served as predefined parameters for mouse study exit.

